

Příloha B

Tezí disertace

---

k získání vědeckého titulu "doktor věd"  
ve skupině věd: **Technických**

# Lab-on-a-Chip systems for point-of-care applications

Komise pro obhajoby doktorských disertací v oboru: **elektrotechnika, elektronika a fotonika**

Jméno uchazeče: **Pavel Neužil**

Pracoviště uchazeče: **Vysoké Učení Technické v Brně**

Místo a datum: **Praha leden 2016**

## **ABSTRACT**

This thesis summarizes the author's activities in the field of microfluidics with a focus on clinical diagnostics during his work in the Institute of Bioengineering and Nanotechnology and Institute of Microelectronics, both A\*STAR Singapore, KIST-Europe in Germany and the Institute of Microelectronics, BUT, Czech Republic between 2004 and 2015. In this thesis, I describe my contributions to the development of portable systems for point of care applications. Different aspects of my activities in the fields of microfluidics and clinical diagnostics were published in 23 peer-reviewed articles with an average impact factor of 8.747.

## **KEYWORDS**

Lab-on-a-Chip, point-of-care diagnostics, microfluidics, infectious diseases, polymerase chain reaction (PCR), reverse transcription (RT), real-time PCR, RT-PCR, silicon micromachining, microfabrication.

# CONTENTS

Abstract .....	2
Keywords .....	2
Contents .....	3
List of figures .....	4
Preface .....	5
1. Introduction .....	6
1.1 Fluid flow in microfluidics channels .....	8
1.2 Chip manufacturing .....	10
2. Development of a Lab-on-a-Chip systems for point-of-care applications .....	11
2.1 Introduction.....	11
2.1.1 Fundamental considerations.....	15
2.1.2 Virtual Reaction Chamber (VRC).....	16
2.1.3 Micro PCR system .....	18
2.1.4 Nano PCR system .....	23
2.1.5 Integrated optical system .....	25
2.1.6 Complete system with sample preparation I, detection of RNA of H5N1 avian influenza virus .....	27
2.1.7 Complete system with sample preparation I, detection of RNA of SARS virus .....	28
2.2 Real-time PCR of 1 <sup>st</sup> generation .....	29
2.3 Real-time PCR of 2 <sup>nd</sup> generation (Universal LOC system) .....	30
2.3.1 LSPR system.....	32
2.3.2 NW system.....	32
2.4 real-time PCR of 3 <sup>rd</sup> generation .....	33
2.4.1 Technical concept .....	33
2.4.2 Applications .....	34
2.5 Other results .....	35
2.5.1 Contactless temperature measurement.....	35
2.5.2 Superheating .....	36
2.5.2.1 DNA release from spores.....	36
2.5.2.2 Physics of overheated VRC .....	36
2.5.2.3 Peptide hydrolysis .....	36
2.5.3 PCR technique development .....	37
2.5.3.1 Multiplexing I .....	37
2.5.3.2 Multiplexing II .....	37
2.5.4 Pyrosequencing .....	38
2.5.5 Other work in microfluidics .....	39
2.5.6 Review .....	40
3. Future work .....	40
4. Conclusion.....	43
5. References:.....	44

## LIST OF FIGURES

Figure 1 Palm sized real-time PCR. ....	5
Figure 2 Original idea how to transform standard biological laboratory into an LOC system .....	6
Figure 3 Bioanalyzer 2100 produced by Agilent with an inset showing their microfluidic chip.....	7
Figure 4 Accu-Check system produced by Roche. ....	7
Figure 5 Bernoulli's Law derivation diagram. ....	9
Figure 6 Simulated profile in channel with rectangular cross section.....	10
Figure 7 PCR principle. ....	12
Figure 8 Reverse transcription PCR (RT-PCR).....	13
Figure 9 Real-time PCR.....	14
Figure 10 Our first idea about the entire system.....	15
Figure 11 Two images overlapping each other of water and oil droplets .....	17
Figure 12 CAD VRC system.....	18
Figure 13 Computer aided design (CAD) of part of a micromachined silicon chip.....	19
Figure 14 Temperature distribution at the silicon chip as modelled by ANSYS.....	19
Figure 15 Temperature measurement and its control. ....	20
Figure 16 Fabricated PCR chip with four samples, here emulated by blue ink. ....	21
Figure 17 IR image of a PCR chip with heater's temperature set to 56, 72 and 95 °C.....	22
Figure 18 PCR amplification curve using continuous fluorescence monitoring .....	22
Figure 19 Melting curve analysis (MCA) a (inset) CE analysis of the PCR product. ....	22
Figure 20 Miniaturized version of the micro PCR system, so called nanoPCR with VCRs .....	23
Figure 21 Continuous fluorescence monitoring using "nanoPCR" system .....	23
Figure 22 RT-PCR RNA of a avian influenza virus H5N1 and extracted amplification curve PCR. ....	24
Figure 23 Fluorescent microscope used for our work with PCR system underneath it. ....	26
Figure 24 CAD drawing of miniaturized fluorescent system. ....	26
Figure 25 Entire view (CAD drawing) at the fluorescent optical system .....	26
Figure 26 Electronic schematic of optical detection system with lock-in amplifier. ....	27
Figure 27 Normalization curve of RT-PCR using RNA of H5N1 avian influenza virus. ....	28
Figure 28 Photograph of a real-time PCR system of first generation. ....	29
Figure 29 Detection of H5N1 avian influenza RNA using real-time PCR system of 1 <sup>st</sup> generation.....	29
Figure 30 Modular LOC system of second generation.....	30
Figure 31 Core of the LOC system of second generation. ....	31
Figure 32 LSPR system. ....	32
Figure 33 CAD image of a system with 64 nanowires (NW). ....	32
Figure 34 Photograph of LOC system of 2 <sup>nd</sup> generation with chip having 64 nanowires .....	32
Figure 35 Real-time PCR of 3 <sup>rd</sup> generation. (A) CAD drawing and (B) fabricated system. ....	33
Figure 36 Results from the real-time PCR system of 3 <sup>rd</sup> generation.....	34
Figure 37 Cross-section of optical part of the system showing light path.....	34
Figure 38 Hand held device of 3 <sup>rd</sup> generation showing detection of Ebola virus RNA. ....	35
Figure 39 A photograph of a glass with 4 VCRs containing nucleotides A, C, G, and T .....	38
Figure 40 Pyrosequencing principle.....	38
Figure 42 Pyrogram (A) and extracted area (B) and peak values (C). ....	39
Figure 41 Princip použitého systému pyrosekvencí.....	38
Figure 42 Fabricated glass wafer with diameter of 100 mm containing 12 chips with ES sensors .....	41
Figure 41 Results from a typical CV scan in 1 mM of K <sub>4</sub> [Fe(CN) <sub>6</sub> ] solution .....	41

## PREFACE

The efforts of myself and my co-workers over 12 years resulted in the smallest real-time polymerase chain reaction (PCR) system in the world to detect pathogens based on their specific RNA or DNA (Figure 1) as is described in this thesis.

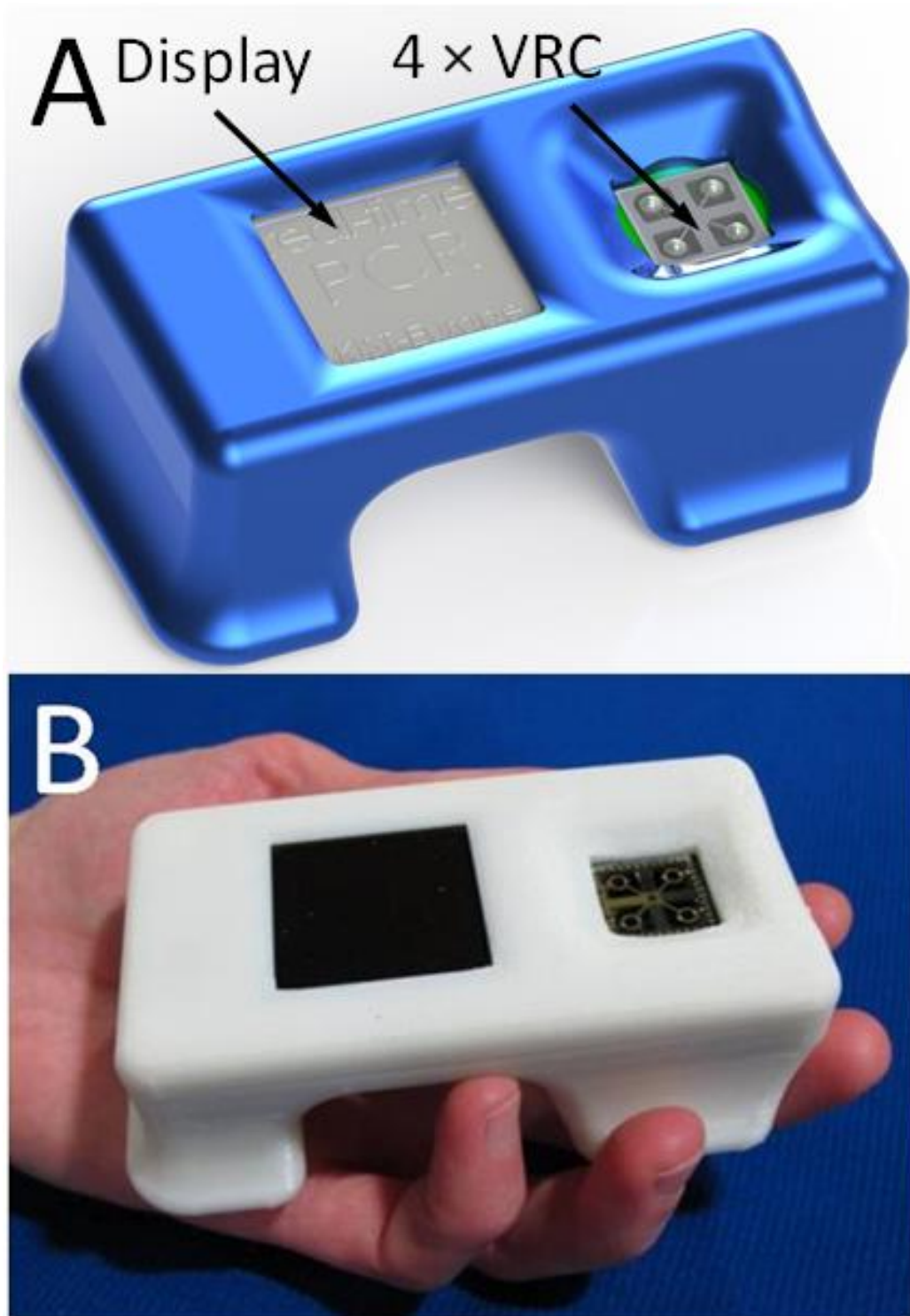


FIGURE 1 PALM-SIZED REAL-TIME PCR.

# 1. INTRODUCTION

New technologies are typically successfully commercialized based on foreseeable market needs for those technologies, especially in the consumer markets; such an example was the entire semiconductor industry. In the field of microfluidics, typical devices created by demand were commercially very successful, for example the micromachined inkjet heads. In comparison to inkjet printing technologies, the microfluidics for bio applications and especially for point of care (POC) applications have been a niche technology for a long time. In my opinion, microfluidics for bio applications was created prior to industry need, due to the availability of aging lines for integrated circuit (IC) manufacturing. These lines were working but already beyond their projected life span so using them cost very little. Nevertheless, their capacity and performance was not sufficient for IC manufacturing any longer. They still were able to perform lithography with a resolution of 1  $\mu\text{m}$  or less but modern IC demanding better performance. These lines were often converted to be able to produce microelectromechanical systems (MEMS) such as pressure sensors, accelerometers, gyroscopes etc. Later on, these lines were not sufficient even for MEMS and started to be used for microfluidic chips. The first fabricated microfluidic device was a chip for a gas chromatograph according to work published in 1979.<sup>1</sup> It was an interesting device which caused some attention of scientists but it did not last for too long. Around 1990, a group of scientists leaded by Andreas Manz in the company Ciba in Switzerland triggered an avalanche of interest in microfluidics. It started with Manz's vision to convert an analytical chemistry into microfluidics (Figure 2). He also introduced the term *micro total chemical analysis system* (microTAS).<sup>2,3</sup> Even at that time he was wondering if these new miniaturized systems were only a short fashion hype or a new technology.<sup>4</sup> Today, this technology is generally called microfluidics, also microTAS or Lab-on-a-Chip (LOC). There is a conference held every year called microTAS with more than 1000 participants. Manz also started a biweekly published journal (originally monthly) called Lab-

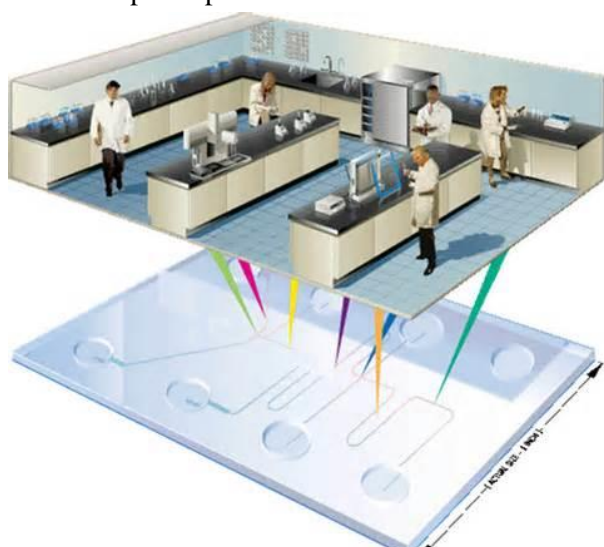


FIGURE 2 ORIGINAL IDEA HOW TO TRANSFORM STANDARD BIOLOGICAL LABORATORY INTO AN LOC SYSTEM (TAKEN FROM INTERNET).

on-a-Chip published by Royal Chemical Society, UK. The journal is considered to be successful and it currently has an impact factor (IF) of 6.115.

It was a bit inadequate calling those miniaturized systems LOC. They cannot work without supporting techniques such as power supplies, pumps, and fluorescent detecting systems. At that point of time, there are two common blue light sources, Ar laser or halide burner. Ar laser weight was 20 kg or more and it was water cooled. Also, its cost of about 20 000 US\$ (\$) and relatively short life span (2000 hours) made it quite



FIGURE 3 BIOANALYZER 2100 PRODUCED BY AGILENT WITH AN INSET SHOWING THEIR MICROFLUIDIC CHIP.

prohibitive. A Halide burner had a life span of only 120 – 150 hours and it was not cheap either. It would be better to call the system “chip-in-a-lab” than LOC. Many times, the adoption of certain groundbreaking technology can only take off when supporting technologies are developed. Microfluidic technology is no exception. For example, the new light sources such as blue LEDs with over 50 000 hours of life span and cost of 0.5 \$ per unit were developed quickly in the 2000s, and this made fluorescent detection technique very affordable to anyone.

Andreas Manz started his work by opening an analytical chemistry text book (as per his own statement) and techniques in individual chapters converted into microfluidics form. The first device was a chip for capillary electrophoresis (CE)<sup>5</sup> including sample dosing,<sup>6</sup> which are used in similar forms till today. The

same principle was also used for on-chip chemical analysis.<sup>7</sup> The next device had a new unique, principle of performing polymerase chain reaction (PCR) in continuous form.<sup>8</sup> It was possible only due to the introduction of microfluidics systems..

Manz’s work has a lot of followers in analytical chemistry, molecular biology, medicine, drug discovery, genetics, forensic science etc. The miniaturized systems were also commercialized, such as Bioanalyzer 2100 by Agilent (Figure 3), where the capillary electrophoresis and thus the analysis of DNA, RNA, proteins or biological cells is conducted in a microfluidics glass chip. The company Roche produces electrochemical sensors based on microfluidics to detect glucose levels or biomarkers for blood coagulation (Figure 4). This system is very cheap as it is mass produced by laser-patterning and laminating a few levels of material together, using a highly automated production line. There are many examples. Nevertheless, it was an uphill battle to convince doctors, who are used to employing certain protocols, techniques and tools, to change their habits and start using new techniques. Step by step, microfluidics started to take over in certain areas, especially where classical approaches are complicated. Researchers also improved new systems and even created new techniques, such as digital PCR (dPCR),<sup>9</sup> which cannot be done by any other means than microfluidics. It’s better to say that without microfluidics, there would be no dPCR. Systems for point-of-care (POC) applications are based on microfluidics.

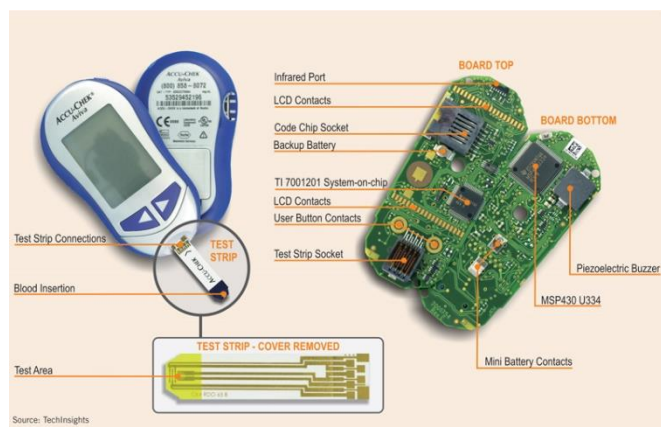


FIGURE 4 ACCU-CHECK SYSTEM PRODUCED BY ROCHE.

Without these techniques, the POC would be too bulky and non-portable. Numerous efforts were done earlier to develop a truly portable POC for diagnostic purposes.<sup>10</sup> The ideal case is to inset a sample of biological material and, after some time, get an answer regarding contamination with virus or bacteria of interest, and ideally without any interaction of an operator. In both of the institutes that I worked for in Singapore, we tried to develop it as well. The Institute of Microelectronics (IME) had a project called BFIG II to detect DNA of interest using sample loading, cell lysis, DNA capturing, its purification, PCR and end point detection using nanowire based sensor. The system was facing a lot of problems, including a complicated design due to the combination of a silicon chip for sample processing and plastic cartridges for fluid reservoirs. The Institute of Bioengineering and Nanotechnology (IBN) had a project called microKIT and it was based on a real time PCR and plastic housing to perform all functions.

A very well-known but non-portable microfluidic system for sample to answer is called GeneXpert, made by Cepheid, Inc. It is capable of detecting the DNA of interest starting from a raw sample. It is truly “sample to answer”, i.e. an operator loads the sample into a plastic cartridge preloaded with lyophilized reagents, adds a dedicated amount of water and presses the “start” button. After an hour or so the GeneXpert displays results. The system was rather costly with the weight of about 20 – 30 kg. It was distributed throughout The Republic of South Africa (RSA), heavily subsidized by the Melinda and Bill Gates foundation. Instead of a typical \$30 000 – 40 000, one unit cost only about \$2000 and the balance was covered by the foundation. Also, a single cartridge preloaded with chemicals cost in RSA only \$6 – 8 instead of a usual \$80, making it very affordable. The aim was to diagnose tuberculosis and AIDS (HIV virus).

Many other efforts were also done, such as protein detection by a system called RapiDx introduced by a group at Sandia National Laboratories where they claim to be able to detect protein-based biomarker in 5 – 10 min.<sup>11</sup> Other systems of interest are metabolite-detecting systems, CD4 cell counters, hematology analyzers and especially nucleic acid analyzers for infectious diseases, environmental monitoring, food safety analysis, forensic science etc. Some of them were commercialized, or at least tried to be.<sup>11</sup> To determine specific nucleic acid presence in the sample using a section of POC system is also my main interest, and the efforts put into the development of a PCR for POC for clinical diagnostics is a dominating part of my thesis. It is introduced by a short description of laminar flow in microfluidic systems.

## 1.1 FLUID FLOW IN MICROFLUIDICS CHANNELS

The motion of viscous fluid substances is govern by the Navier–Stokes equations. This set of general equations can be used to model various flows of compressible as well as incompressible fluids. Most micro fluidic devices for POC applications use steady incompressible fluids, i.e. liquids. They can be driven within the microfluidic devices either by pressure (Poiseuille equation) or using electrokinetic forces.



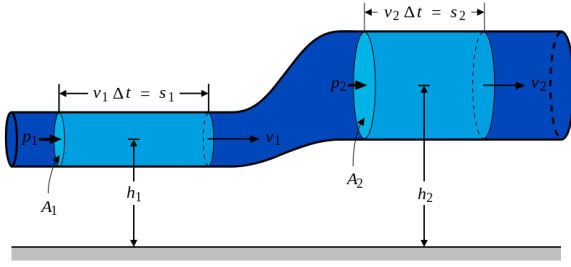


FIGURE 5 BERNOULLI'S LAW DERIVATION DIAGRAM.  $V_1$  AND  $V_2$  ARE FLUID VELOCITIES,  $H_1$  AND  $H_2$  ARE HEIGHTS,  $P_1$  AND  $P_2$  ARE PRESSURES,  $A_1$  AND  $A_2$  ARE PLUGS' AREAS AND  $\Delta T_1$  AND  $\Delta T_2$  ARE THEIR LENGTHS.

Fluid flow in pipelines follows the Bernoulli principle of energy balance, which declares that energy anywhere in the pipeline is the same. It mathematically combines fluid pressure, its velocity and pipe geometry. It also assumes that this fluid has a constant, specific mass, which means it is incompressible. (Figure 5). It also ignores losses in a pipeline due to friction applicable only to incompressible fluids (liquids).

The Bernoulli equation<sup>12</sup> for liquids in microfluidic systems is further simplified as changes in liquid height are marginal and they do not play any significant role.

The parameter which defines the character of liquid flow is called the Reynolds number and it is defined by:

$$Re = \frac{LV_{AVG}\rho}{\mu}, \quad (1)$$

where  $L$  is length,  $V_{AVG}$  is average liquid velocity,  $\rho$  specific mass and  $\mu$  its viscosity.  $Re$  greater than 2000 defines the turbulent flow type while  $Re$  smaller than 100 means laminar flow type. Typical values of  $Re$  in microfluidics are 1 or smaller, thus the flow type in microfluidic channels is always laminar. It has advantages and disadvantages. The results of liquid processing with laminar flow are easily predictable but there is no liquid mixing and that results in complications in chemical or biochemical reactions as they are only driven by diffusion and thus rather slow.

Moving liquids or their components from place to place can be done in principle by two means; pressure- or electric-field-driven.

Pressure driven is rather simple. It is good to have a look at the pressure drop due to liquid velocity. The volume liquid velocity  $Q$ , length of cylindrical tube, dynamic viscosity of the liquid  $\mu$ , radius of the tube  $r$  and pressure difference between beginning and end of the tube  $\Delta P$  is described by the Hagen-Poiseuille equation:

$$\Delta P = \frac{8\mu L Q}{\pi r^4}. \quad (2)$$

This equation is valid for a cylindrical tube but it can be easily converted into any other shape as there is a tube cross section in the Eq. (2). Liquid control by pressure is convenient but due to a small cross section in the channel, the liquid flow rate has to be small to keep the  $\Delta P$  at a reasonable level. Another unwanted effect is inhomogeneity inside the channel (Figure 6)<sup>13</sup> due to friction between the walls and the liquid. Nevertheless, this method is widely used and researchers employed many different pumps. The most popular are syringe pumps. The syringe is filled with a suitable liquid, its piston is controllably

pressed by stepper motor and that pushes the liquid out from the syringe into the tube connected to the syringe. Assuming no air bubbles, the volume pushed from the syringe is the same as the volume entering the microfluidic channel.

Based on the Hagen-Poiseuille equation, i.e. known liquid viscosity, its flow and the cross-section of the microfluidic channel, we can calculate corresponding pressure difference. It is extremely important as the  $\Delta P$  could be so high that the microfluidic chip would be overloaded with it and not be able to handle it. It is not as severe as with big pipelines, but we

do have to keep the pressure drop at a reasonable level. If the calculated pressure is too high, the microfluidic chip has to either be redesigned or the flow rate lowered.

Another option of fluid moving or pumping is based on electrokinetic force. This method does not play any significant role in classical pipelines. It is important that the surface properties and the electrical double layer formed at the surface of the tube (channel) can influence the entire tube volume. This happens in microfluidics, where the distance from the channel surface to its center can be in tens of  $\mu\text{m}$  or even smaller. The electrokinetic force pumping such as osmotic is often more interesting than the pressure driven pumping. First of all, there is no extreme pressure drop and we can move only certain compounds from the fluid, thus separate them from each other and subsequently analyze them, as was done in earlier mentioned capillary electrophoresis.

## 1.2 CHIP MANUFACTURING

As I wrote in the introduction of this thesis, chips for microfluidics were originally made using production lines for integrated circuits. Silicon as a typical substrate has excellent properties, such as an easy manufacturing process, high thermal conductivity, but for applications where high voltage is required, its electrical conductivity makes it unsuitable. Numerous researchers from the semiconductor industry refused to believe it and they tried to develop a capillary electrophoretic (EC) chip using silicon only to find out that indeed it is practically impossible to create a pinhole-free layer which can withstand 10 – 30 kV, and they had to switch to glass. Even though silicon is a wonderful material, its technology is well-known and established, and the researchers were forced to start working with a more open mind and not to be confined into the old way of thinking that silicon can be used for everything. Gradually, glass became the material of choice, and especially plastic such as polycarbonate, polymethylmetacrylate (PMMA), and others. Of course, it has been known for a long time that plastics can be produced by extremely cheap methods. It is only in the last few years that researchers were able to treat plastic surfaces to make the material competitive and it seems now that plastic will prevail.

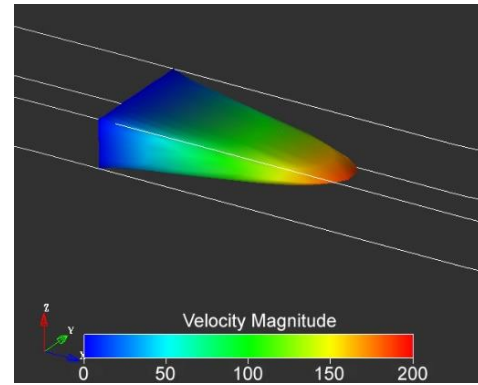


FIGURE 6 SIMULATED PROFILE IN CHANNEL WITH RECTANGULAR CROSS SECTION CREATED BY SOFTWARE COVENTORWARE.

Besides old IC lines, there were also lines for digital versatile disc (DVD) manufacturing. Their sale was decreased and it is only a matter of time till the lines will be shut down. SONY Inc. has one line in Austria near Salzburg and it has been either partially or fully converted into the fabrication of microfluidics chips. The commercialization push of centrifugal force based micro fluidics devices are partly came from the interests of CD/DVD manufacturers.

Fabrication of plastics is of course very different from silicon or glass processing. Plastics are processed by hot embossing, injection molding, casting and vapor deposition. Most commonly used materials are PMMA (plexiglas), polycarbonate (PC), polydimethylsiloxane (PDMS) and parylene. Another material of interest for microfluidic applications is paper.<sup>14</sup>

My major research interest in the last 10 years was the development of infectious disease diagnostic tools with samples processed at the glass surface without any surface patterning based on my philosophy “*there is beauty in simplicity*”.

## 2. DEVELOPMENT OF A LAB-ON-A-CHIP SYSTEMS FOR POINT-OF-CARE APPLICATIONS

### 2.1 INTRODUCTION

My professional career started in the area of semiconductor manufacturing technology, such as complementary metal oxide semiconductor (CMOS), power metal oxide semiconductor field effect transistor (MOSFET), power bipolar junction transistors (BJTs) and later on I concentrated on chemical sensors and microelectromechanical systems (MEMS). In IME, Agency for Science Technology and Research (A\*STAR), Singapore, I was partially involved in Biosystems Focus Interest Group I (BFIG I) project where we developed the micromachined PCR system combined with capillary electrophoreses (CE) as PCR product end point detection method. Once I joined IBN, A\*STAR, in Singapore about 12 years ago, I fully concentrated on medical devices while taking advantage of my previous experience and knowledge in semiconductor and MEMS processes.

Before I joined IBN, there was a crisis through the whole of Asia related to the spreading of a severe acute respiratory syndrome (SARS) virus. A few thousand people around the world died and Singapore was the second most affected place by the virus. This was the reason why we decided to develop a simple, easy-to-use and economical system to detect pathogen presence based on their DNA or RNA sequence. The DNA can be detected directly by the PCR<sup>15</sup> while the RNA has to be at first reversely transcribed into a complementary DNA (cDNA) by a method called reverse transcription (RT) and thus the entire process has name reverse transcription PCR (RT-PCR).

The PCR method was first published in 1983 by Kary Mullis. What was interesting that he “only” used a sequence of known steps, thus achieving one of the greatest inventions of the last century. Rightfully, he was awarded with Nobel Prize for his invention in 1993 for chemistry. PCR is a phenomenal method revolutionizing many fields, such as medicine, genetics, forensic science, paternity recognition, genealogy etc. The Nobel Prize had two parts, the PCR itself and the extraction of an enzyme capable of surviving in high temperatures. Mullis used Taq polymerase enzyme from the bacteria *Thermus aquaticus*, which is able to survive in hot water.

Why is PCR so great anyway? PCR can be also called a highly specific biological or biochemical replicator of DNA (Figure 7). The PCR solution also known as a “PCR master mix” has to contain sample of DNA which we are trying to replicate, polymerase enzyme, oligonucleotides (primers) specific to the DNA sequence we are looking for, free nucleotides adenine (A), thymine (T), cytosine (C) and guanine (G), bivalent cations  $Mg^{2+}$  or  $Mn^{2+}$  and buffer solution to stabilize the polymerase and correct pH buffer.

PCR itself is a sequence of temperature cycling steps<sup>16</sup> of a DNA template in PCR master mix. The first step is to heat up the solution at a high temperature, typically  $\approx 95\text{ }^{\circ}\text{C}$  to activate the polymerase enzyme. During that step, each molecule of a double stranded DNA (dsDNA) “melts” into two molecules of single strand

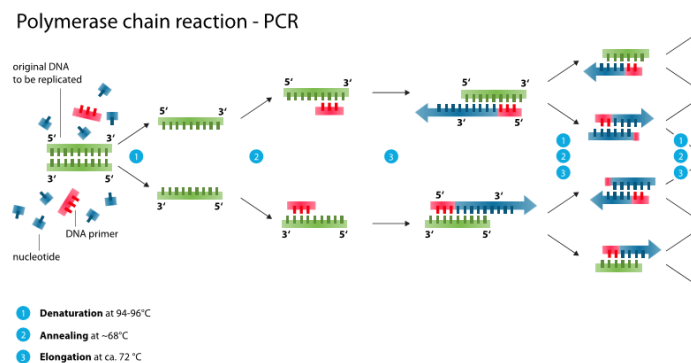


FIGURE 7 PCR PRINCIPLE.

DNA (ssDNA). This step is also called denaturation. The master mix is then cooled to an annealing temperature (between  $\approx 50\text{ }^{\circ}\text{C}$  and  $\approx 60\text{ }^{\circ}\text{C}$ ) when primers anneal to the ssDNA, assuming that there is a DNA template with a sequence complementary to the primers in the master mix. In the next step, the solution is heated up to  $\approx 72\text{ }^{\circ}\text{C}$  and assuming the pH of the solution is favorable, in the presence of bivalent salt, polymerase enzyme and free nucleotides A, C, G, and T, both the DNA sequences are completed into two dsDNAs. These three temperature steps are repeated 30 – 40 times. For example, if they are repeated 40 times, one can expect that the number of DNA copies in the sample would be then replicated  $2^{40}$  times. This is an incredible number of almost  $1.1 \times 10^{12}$ . In reality, the number of replicas is not that high, as during the PCR the master mix gets depleted and the replication stops. Also, the PCR efficiency is never 100%; the real number of replicas is smaller. Nevertheless, the number of replicated copies is still phenomenal. The PCR method also has a high specificity because if there is no DNA specific to the primers, no replication occurs. Once the PCR is completed, the product (if there is any)

has to be detected by its analysis. It is typically done by hybridization using suitable targets or by electrophoresis, either using gel or a capillary. This short description shows the power of the technique.

In our application, we need to diagnose the presence of a certain type of virus that has its genetic information coded in RNA and not in DNA. To do this, first we had to prepare the specific cDNA.<sup>17</sup> In

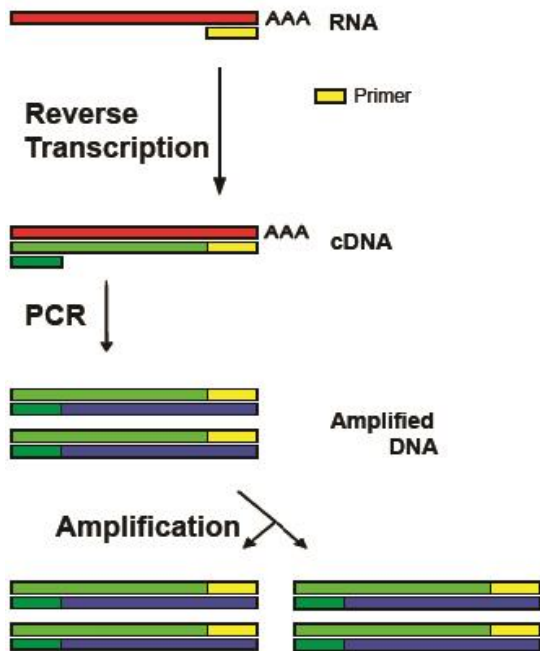


FIGURE 8 REVERSE TRANSCRIPTION PCR (RT-PCR)

the presence of an enzyme called reverse transcriptase in a suitable environment and at temperature  $\approx 60^\circ\text{C}$ , the RNA gets reverse transcribed into cDNA (Figure 8). Once the genetic information is in the format of cDNA, these DNA molecules can be replicated and their number can be increased to a detectable level using the PCR process. As mentioned before, the DNA product (call amplicon) presence after the PCR has to be confirmed by another end-point method. There are a few methods, such as hybridization and electrophoresis, either gel-based or capillary-based. Gel-based electrophoresis is considered a standard method. It is economical, requiring only a sheet of agarose gel, a high voltage (15 – 30 kV) power supply, ethidium bromine for staining and an optical reader.

Regardless of which end-point detection method is used, there are two drawbacks. The obtained result is only qualitative as it does not give us any information on how many copies were presented in the sample at the beginning, i.e. no quantitative information can be achieved. The second drawback is the necessity of sample manipulation after the completion of PCR as the sample has to be transferred from the PCR system to another one to detect the amplicon presence and its properties.

In 1993, a method of quantitative PCR (qPCR) was published by R. Higuchi.<sup>18</sup> He added fluorescent intercalating dye called SYBR-Green I into the PCR master mix. This dye does not produce any fluorescence in a water environment. Once it binds to the dsDNA, which is hydrophobic, SYBR-Green I starts emitting green light when illuminated by blue light. Optimum excitation wavelength is  $\approx 490\text{ nm}$  and maximum emission wavelength is around  $\approx 515\text{ nm}$ . The amplitude of fluorescence is proportional to the number of dsDNA copies in the solution. During the PCR sequence, the fluorescence amplitude is measured in each cycle at the end of the extension step at  $\approx 72^\circ\text{C}$ . Once the measurement is completed, one can create a curve with a cycle number at X-axis and fluorescence amplitude at Y-axis typically having a shape of a sigmoid. The fluorescence monitoring is conducted during the PCR in real-time, thus this method has also named “real-time PCR”.

This method is also quantitative. We can perform a set of measurements with known number of copies of DNA template. Typically the range of DNA copies differs in many orders of magnitude,<sup>19</sup> from 1 (statistically most probable number) to at least 10 000 or more (Figure 9). Once the PCRs are completed, we plot the PCR amplification curves and set an artificial threshold value. The intercept values of the threshold and the PCR amplification curve is then plotted as function of log (concentration). This is called PCR standard curve and it is a base for further quantification of samples with an unknown number of DNA copies. Slope of this curve shows the efficiency of PCR amplification. Once we perform PCR with a sample containing unknown number of copies of the DNA template, we create a PCR amplification curve, determine the threshold value and from the normalization curve we can conclude what the DNA number of copies in the original sample was.

This quantitative PCR can also be used to determine the efficiency of reverse transcription (RT) by comparing different samples or different RT conditions by determining DNA copy numbers by the real-time PCR method.

The SYBR-Green I produces fluorescence only in presence of dsDNA. During the PCR process, each molecule of dsDNA melts at melting temperature ( $T_M$ ) into two molecules of ssDNA and at that moment the SYBR Green I stop exhibiting fluorescence properties. The value of  $T_M$  depends on the DNA length (number of base pairs) and its composition. Once the PCR is completed, typically a melting curve analysis (MCA) is performed. The sample is slowly warmed up from  $\approx 72$  °C to  $\approx 93$  °C while its fluorescence amplitude is monitored. We then plot the negative derivative of  $dF/dT$  as function of temperature. There should be a peak of this derivation at approximately predicted  $T_M$  of the expected amplicon. I wrote “approximately” on purpose as the exact value of the  $T_M$  is affected by the master mix composition, bivalent salt concentration etc. and it can vary by a few °C. Single peak at the graph  $-dF/dt = f(T)$  shows that there is only a single amplicon in the PCR product. This method is not as precise as capillary electrophoresis but its great advantage is its convenience. The sample is analyzed immediately once the PCR is completed using the same system with no sample manipulation. Typically, the MCA is part of the PCR protocol.

Typically, for any clinical samples there should at least be three tests conducted concurrently: a clinical sample, negative control and positive control. The sample for negative control is only water with no template to determine if there is any sample to sample cross-contamination. It should exhibit no amplification curve. The positive control sample contains either RNA or DNA, depending on the

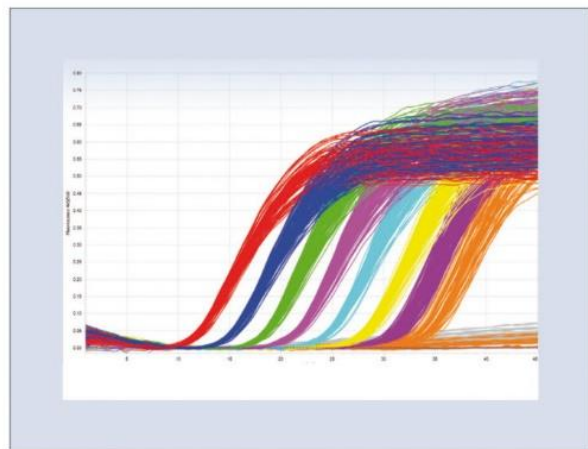


FIGURE 9 REAL-TIME PCR.



template of the clinical sample. The purpose of positive control is to verify that the PCR or RT-PCR process was successfully conducted and everything, such as master mix composition and (RT) PCR protocol, was successfully conducted. Both “false positive” or “false negative” results can have severe consequences thus their elimination is an important step.

### 2.1.1 FUNDAMENTAL CONSIDERATIONS

We decided that the new system for point-of-care applications to be developed has to have the following properties (Figure 10):

- Ability to detect the presence of viruses or bacteria using the real-time PCR (or RT-PCR) method
- Economical and thus affordable in countries with lower gross domestic product (GDP) per capita
- Disposable parts getting into contact with the sample to avoid sample to sample cross contamination
- Efficiency of either DNA or RNA has to be comparable with commercially available systems
- Faster than current systems
- Can perform both PCR and RT-PCR
- Small size for easy transportation
- Powered by 12 V battery

I further elaborate on the points in the following. We worked in South-East Asia and we wanted to develop a simple diagnostic system, affordable for small clinics in regions such as rural areas of Indonesia, Thailand, Vietnam, Laos, and Myanmar, etc. During my previous assignment in the Institute of Microelectronics, A\*STAR, Singapore, we formed a consortium “Bioengineering Focus Interest Group” (BFIG) and developed an interesting microfluidic PCR chip with a small reaction chamber, based on the silicon micromachining technique, glass to silicon bonding, ultrasonic drilling etc.

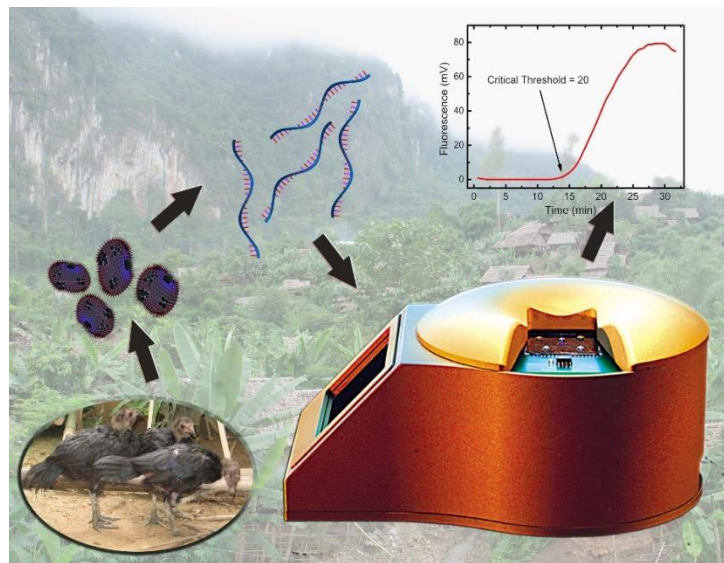


FIGURE 10 OUR FIRST IDEA ABOUT THE ENTIRE SYSTEM IS SHOWN HERE. WE WOULD EXTRACT VIRUS FROM A BIOLOGICAL SAMPLE FROM A POULTRY, RELEASE ITS RNA AND USING RT-PCR TO DETECT ITS PRESENCE.

We were able to warm up the sample rather quickly but its cooling was a problem. Its cost was also prohibitive, especially since the design was not optimized and the PCR’s temperature sensors had to be individually calibrated.

Another problem was not technical and turned out to be the most severe from the issues described above, and that is the end users’ habits. I am 100 % positive that we can clean the silicon PCR chamber

using a classical piranha solution consisting of  $\approx 30\%$   $\text{H}_2\text{O}_2$  and  $\approx 97\%$   $\text{H}_2\text{SO}_4$  at a temperature of  $\approx 120^\circ\text{C}$  so well that not a single molecule of RNA or DNA would stay there. Unfortunately, what is not possible is to convince potential users about this. They require a disposable system; one-time use only. We had no choice except to accept it; thus, we decided that anything which comes into contact with the DNA/RNA sample has to be disposable. This was the first lesson to learn considering any real-world applications of such a device.

It is a given that convincing scientists to start using different systems is not a simple task. They are used to a certain standard and without giving them something extra, they are not going to switch to new systems, technologies or protocols. One of the key aspects is that the new solution has to be at least as good as the old solution, with some improvements. The efficiency of the PCR amplification had to be at least the same as that of commercial products.

Of course, the new system had to be fast as well. We expected that these newly developed systems would also be used at airports. Travelers showing signs of fever during the SARS outbreak could be tested in 10 – 15 min to confirm the infection.

We also decided that the system had to be able to detect RNA, which meant performing RT-PCR. This requirement is obvious, as viruses such as SARS, avian influenza of H1N5 or H7N9 have their genetic information coded in the RNA and not in the DNA. From an engineering point of view, that does not matter at all. PCR starts with a hot start step. An RT-PCR has an additional RT step before the hot start, consisting of keeping the sample at  $\approx 61^\circ\text{C}$  for few min. Engineers solve this just by adding one extra step into the temperature controlling program. Molecular biologists know that a sample containing RNA is not simple, as RNA is rather unstable compared to the DNA, and the system has to be rigorously tested to find out if the RNA stability is sufficient.

The system had to be portable, which means its weight has to be significantly less than 1 kg.

Finally, there was a requirement to power the system with a 12 V DC power supply. Different countries have different effective AC voltage standards in distribution networks, from 100 V in parts of Japan to 230 V in Europe. There is one voltage practically universally available throughout the entire world, which is the 12 V DC supplied by a car battery.

### 2.1.2 VIRTUAL REACTION CHAMBER (VRC)

I like simple things as they tend to be reliable. Stationary systems are also more trustworthy than movable ones. Also, complicated systems have a much higher chance of failure than simple ones. “Simplicity” was the keyword we decided to follow. My co-worker in IBN, Juergen Pipper, was involved in the development of surface-based microfluidics in his previous assignment at University of Jena, Germany.<sup>20</sup> They used surface acoustic waves (SAW) to move droplets from station to station in form of a virtual reaction chamber (VRC). Juergen’s field is surface chemistry and I am an electrical



engineer, thus our collaboration was fruitful. He was in charge of sample handling and processing and I was in charge of the hardware and software. The system developed in Jena was interesting, but I did not much like the principle of SAW. It is in my opinion too complicated as it requires fine line lithography and metal etching (or lift-off process). Also, the substrate has to have piezoelectric properties such as the most commonly used LiTaO<sub>3</sub>, LiNiO<sub>3</sub> or special cuts of Quartz and none of them are cheap or easy to process. Since there was a requirement

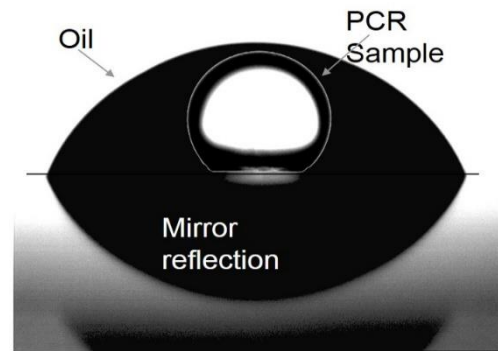


FIGURE 11 TWO IMAGES OVERLAPPING EACH OTHER. INSIDE IS THE WATER DROPLET COVERED WITH OIL AT HYDROPHOBIC COATED GLASS SURFACE.

that anything getting into contact with the sample had to be disposable, SAW materials were out of question. We therefore decided to use glass. It is cheap, can be processed by the same mass production techniques as silicon and the surface chemistry at SiO<sub>2</sub> surface is well-known and rather simple. Our system can be then considered as one of open surface microfluidics (OSM). Once the SAW principle was ruled out, it was clear that the sample would either be 100% stationary or had to be moved by another principle. Originally, we used glass substrate. We deposited a gold layer with thin film chrome as adhesion layer and lithographically patterned them to form heater and sensor. Soon we realized that it was not a good idea. The substrate thickness was  $\approx 0.5$  mm, its machining was difficult compared to that of silicon and it was close to impossible to make thermally isolated structures. Once we heated up one structure, we in fact heated up the entire chip. Heat transfer through the glass was slow and overall the performance was greatly unsatisfactory. We also did not particularly like the fact that every single chip required gold/chrome sputtering, lithography, etching, dicing the wafer into individual chips, mounting the chips to the printed circuit board and calibrating the integrated temperature sensors.

We decided then to take advantage of cheap glass substrate as well as of the high performance micromachined silicon. Silicon has excellent thermal properties, its thermal conductivity is  $\approx 100 \times$  greater than the one of glass. Its micromachining is well known and we could create thermally isolated structures. Also I had a number of years of experience of development of a micromachined bolometer in my previous institute of IME, where I was in charge of a team developing an uncooled bolometer-based infrared camera. Principles of both systems are similar, both have to be heated up and cooled down. Or course, bolometer is much more demanding from thermal design and optimization point of view.

We proposed a system consisting of a micromachined silicon chip integrated with heater and a temperature sensor. The sample in the form of a VRC would be separated from the silicon chip by a microscopic glass cover slip. This glass with typically thickness of 170  $\mu\text{m}$  would be placed on the silicon chip and thermally connected with the silicon chip by a thin layer of a mineral oil.

We used a sample with a volume between  $\approx 0.1 \mu\text{L}$  and  $\approx 5 \mu\text{L}$ . This range was found to be practical. Handling samples smaller than  $\approx 0.1 \mu\text{L}$  is complicated and it is also the smallest volume one can dispense by manual pipette. Volumes greater than  $\approx 5 \mu\text{L}$  had large heat capacities, thus the system was too slow.

The microscope glass cover slip was coated with fluorosilane (heptadecafluoro-1,1,2,2-tetrahydrodecyl)trimethoxysilane, (tridecafluoro-1,1,2,2-tetrahydrooctyl)trichlorosilane (FOTS) or 1H, 1H, 2H, 2H-perfluorodecyl-triethoxysilane (FAS-17), typically by a chemical vapor deposition (CVD) process at temperature of  $\approx 150^\circ\text{C}$ . The water contact angle at this surface was as high as  $\approx 115^\circ$  and mineral oil type Sigma M5904 exhibited an angle of  $\approx 65^\circ$  (Figure 11). These

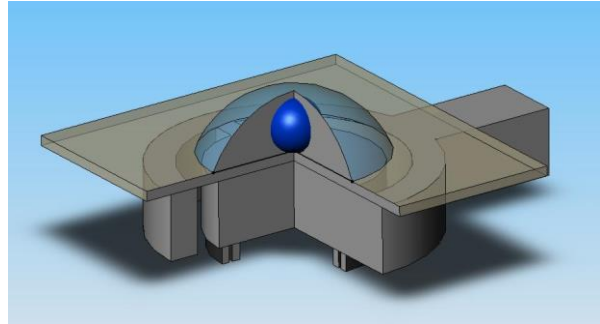
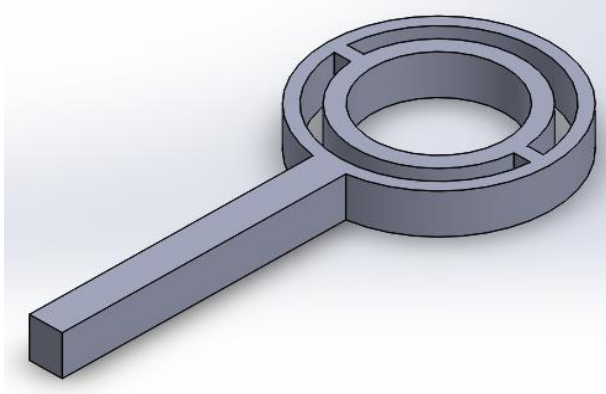


FIGURE 12 CAD VRC SYSTEM.

hydrophobic and oilphobic properties ensured that both liquids did not spread around and stayed where we dispensed them. The water-based sample was either pipetted into an oil droplet with typically volume  $3\times$  greater than that of the sample. Surface tension of both liquids with their ratio of 1:3 resulted in self-aligned system with the water sample in the center of the oil droplet. The cross section through the water-based sample is shown in Figure 11. It is a photograph of an oil droplet at the glass surface, superposed with an image of water droplet in a glass cuvette. We also drew a proposed system using computer aided design (CAD) software (Figure 12).

### 2.1.3 MICRO PCR SYSTEM

As I wrote in the previous chapter, we assumed that glass with a thickness of  $170 \mu\text{m}$  will be placed at the silicon chip made by micromachining technique (MEMS) as it is schematically shown in Figure 13. The silicon chip should have the heater and the resistor from the backside made of sputtered or evaporated metal. This metal had to fulfill few functions thus choosing it was rather critical. We planned to use it as resistive temperature detector (RTD) type of sensor so its temperature coefficient of resistance (TCR) was an important parameter. It should also serve as a heater and we planned to use relatively low voltage power supply so we needed material with low sheet resistance value. Also, processing this material should be simple. Finally, we needed to solder the fabricated chip to the supporting printed circuit board. We did not know how long it would take between the chip fabrication and its soldering, so the metal should not be easily oxidized. Only platinum and gold fulfilled these requirements. Gold processing was significantly easier than that of platinum so we chose gold as heaters' and sensors' material.



**FIGURE 13 COMPUTER AIDED DESIGN (CAD) OF PART OF A MICROMACHINED SILICON CHIP. BOTH HEATER AND SENSOR IS PLACED AT THE BACKSIDE OF THE SILICON. THIS SILICON SHAPE INCLUDING THE AIR GAPS ENSURE MINIMAL TEMPERATURE GRADIENT ALONG THE INNER DONUT SHAPE REQUIRED FOR HIGH PCR PERFORMANCE.**

Our co-worker required that we control temperature with precision of  $\pm 0.1$  °C and have temperature non-uniformity across the heater also  $\pm 0.1$  °C. Later on, we found out that these strict requirements were not necessary but at that point of time we did not know it. We therefore designed the silicon chip in a double donut shape (Figure 13). The thermal properties of the shape were modeled using finite element analysis (FEA) software ANSYS and after several optimizations, we found that indeed the temperature along the inner donut in a steady state is practically identical (Figure 14). We also performed transient analysis and found that the

structure should have a very fast heating/cooling rate of about a few tens °C/s. Heating is almost always easier than cooling and it is conducted by dissipated Joule heat  $P$  in the structure:

$$P = \frac{V^2}{R}, \quad (3)$$

where  $V$  is voltage at the heater and  $R$  its resistance. Solving the thermal heat balance equation gives us a heating rate:

$$\Delta T = \frac{P}{H}, \quad (4)$$

where  $H$  is system heat capacity. We calculated the value of  $H$  and assumed that perhaps we might not need active cooling thus only passive cooling should be sufficient. Passive cooling means that with



**FIGURE 14 TEMPERATURE DISTRIBUTION AT THE SILICON CHIP AS MODELLED BY ANSYS. WE ASSUMED FOUR HEATERS WITH TEMPERATURE SET TO  $\approx 56$  °C, TWO HEATERS AT  $\approx 72$  °C A ONE AT  $\approx 93$  °C.**

heating power off, the system temperature quickly equalizes with ambient temperature by heat dissipated from the VRC to the system via a silicon beam between the heater and the frame of the silicon chip. It should be possible as silicon is known as a highly thermally conductive material with its thermal conductance  $\lambda_{si}$  of 157 W/m·K. In such a case, the system cooling would follow an exponential equation of the first order controlled by system thermal time constant  $\tau$ .

$$\tau = \frac{H}{G}, \quad (5)$$

where  $G$  thermal conductance of the silicon beam. Its thermal conductance can be derived using the equation:

$$G = \frac{wt}{L} \lambda_{Si}, \quad (6)$$

where  $w$ ,  $t$ , and  $L$  are beam width, thickness and length, respectively. A fast system with a small  $t$  has to have a small heat capacity and/or a high value of  $G$ . The latter one gives us a problem as systems with high values of  $G$  are also power demanding:

$$P = G\Delta T, \quad (7)$$

thus the solution of having a high  $G$  is not practical for POC systems. Having a small  $H$  is a better option. This was discussed earlier during the section regarding design considerations. We decided that we would try to keep the heat capacitance and thus the sample size minimal to achieve ultimate heating/cooling rates.

The layout of the heater had a hole in its center. We knew from the very beginning that we had to be able to measure fluorescence amplitude from the sample as function of a cycle number, i.e. performing the real-time PCR. We decided that the integrated optical system has to be underneath the sample and that is why we designed heater with the hole in its center. We knew that minimal number of samples is 3 or 4. One has to be as negative control, one as positive control and one or two with clinical samples. We then designed the chip to accommodate four samples a time. Temperature distribution at four heaters was simulated and we found that the micromachined silicon with thermal isolation done by air gaps was an excellent solution as we practically did not observe significant cross talk (Figure 14).

The electronic circuit for heating and temperature sensing was rather simple. The dissipated power was controlled using pulse-width modulation technique with a closed loop system, using a proportional integrative derivative (PID) control method. The dissipated power

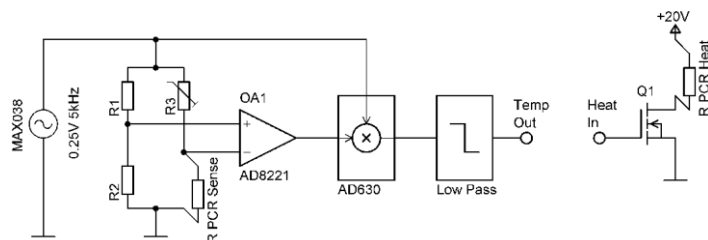


FIGURE 15 TEMPERATURE MEASUREMENT AND ITS CONTROL.

was controlled by switching on and off the transistor Q1 (Figure 15). We chose the PWM method due to its power efficiency. Once the Q1 transistor was on, full power was used to heat up the heater. When the transistor was off, there was no power dissipation in the heater. The switching on/off had to be much faster than the  $\tau$  of the system. It was an easy task as the  $\tau$  was expected to be between  $\approx 0.2$  and  $\approx 2$  s and we used a square wave signal with 10 kHz pilot frequency for the PWM.

First, the temperature sensing was done using a conventional DC powered Wheatstone bridge. Its output signal was proportional to its DC bias voltage. We used 5 V to power it and found that the dissipated

power in the sensor warmed up the silicon heater by at least  $\approx 3$  K. The only solution was to lower the bias voltage for the Wheatstone bridge without suffering the temperature measurement sensitivity. We therefor decided to power the bridge by an AC voltage with demodulator and low pass filter at the bridge output. This system is called lock-in amplifier and it can also be considered is as very narrow band pass amplifier, i.e. selective to the AC signal frequency used to power the bridge.

Once the original consideration was completed we fabricated the chips. We used doubles sided polished silicon wafers with crystallographic orientation of  $\langle 100 \rangle$ , diameter of  $\approx 100$  mm and thickness of  $\approx 450$   $\mu\text{m}$ . First we deposited low stress layer of  $\text{SiO}_2$  with thickness of  $\approx 1$   $\mu\text{m}$  using plasma enhanced chemical vapor deposition (PECVD) technique followed by  $\approx 20$  nm thin layer of chrome for adhesion of subsequent  $\approx 200$  nm thick layer of gold. Both metal layers were deposited by evaporation in high vacuum using electron gun power source. We used such a thin layer of Cr to ensure that the resulting TCR is practically the one of Au with Cr only marginally affecting it. We performed contact lithography and removed unwanted Au and Cr layer using backsputtering or ion milling process. Photoresist was removed and a layer of  $\text{SiO}_2$  was deposited second times now to mechanically protect the Au/Cr layer. We performed second lithography and using  $\text{HF}/\text{NH}_4\text{F}$  solution with ratio of 1:6 the contact pads for further gold soldering were opened. We removed photoresist and using 3<sup>rd</sup> lithography this time with photoresist with the thickness of  $\approx 10$   $\mu\text{m}$ . Next step was again  $\text{SiO}_2$  etching to open access to silicon chip and by deep reactive ion etching (DRIE) we etched through the entire silicon chip. Once the photoresist was removed and the chips were overall cleaned we soldered them to the custom made PCBs and they were ready for testing.

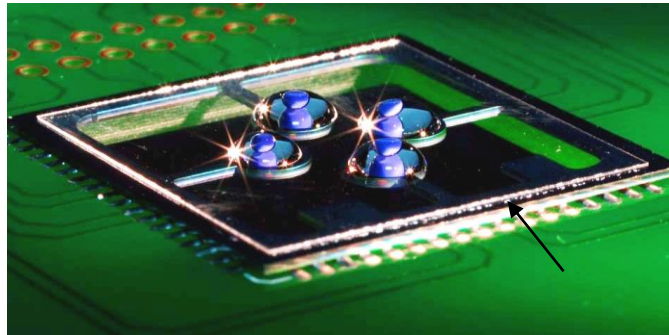


**FIGURE 16** FABRICATED PCR CHIP WITH FOUR SAMPLES, HERE EMULATED BY BLUE INK. THE CHIP IS MOUNTED AT THE PCB AND SAMPLES ARE SEPARATED FROM THE CHIP BY GLASS COVER SLIP WITH THE THICKNESS OF  $\approx 170$   $\mu\text{m}$ .

The fabricated chip (Figure 16) had a size of  $\approx 24$  mm  $\times$  24 mm. We placed a microscope cover slip with a size of  $\approx 22$  mm  $\times$  22 mm and a thickness of  $\approx 170$   $\mu\text{m}$  on the silicon chip. Glass was only placed on the silicon chip and we dispensed a few  $\mu\text{L}$  of mineral oil M5904 (Sigma) at their interface. Due to capillary forces oil was sucked in between them and temporarily “glued” the glass to the silicon chip. This thin layer of oil also served as thermal “bridge” between both materials. One can see droplets of oil pushed out at the interface glass-silicon as pointed by an arrow in Figure 16.

We used an infrared camera operating with wavelength lengths in range from 8 to 14  $\mu\text{m}$  check the temperature non uniformity at the glass (Figure 17). Next we measured thermal parameters of fabricated chip and we were ready for PCR.

We first tested this new PCR concept using fragment of human genome called glycerin aldehyde 3-phosphate dehydrogenase (GAPDH) with length of 208 base pairs (bp) using 940 copies of the template in the master mix solution. Specific oligonucleotides were: forward 5'-CTCATTTCCTGGTATGACAACGA-3' and reverse 5'-GTCTACATGGCAACTGTG-AGGAG-3', both supplied by Research Biolabs,

Inc. The PCR master mix was prepared in volume of  $\approx 50 \mu\text{L}$  based on protocol by its manufacturer, Qiagen, Inc. The PCR master mix was meant for standard non quantitative PCR. We then added solution

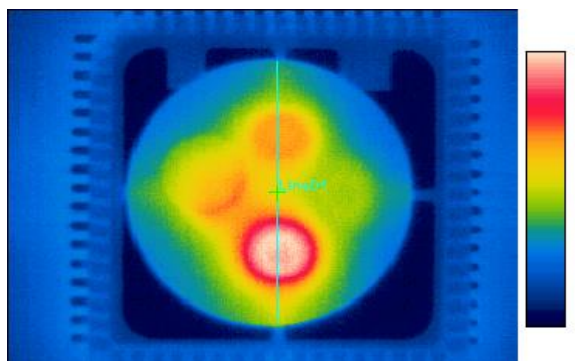


FIGURE 17 IR IMAGE OF A PCR CHIP WITH HEATER'S TEMPERATURE SET TO 56, 72 AND 95 °C, RESPECTIVELY.

of SYBR Green I supplied by Invitrogen, Inc. in ratio of 1:10000 and also bovine serum albumin (BSA) supplied by Carl Roth, Inc. with final concentration of  $\approx 1\%$ . Presence of SYBR Green I allowed us to monitor the PCR in real-time and BSA avoided DNA template to incubate at the glass surface and thus inhibit the PCR.

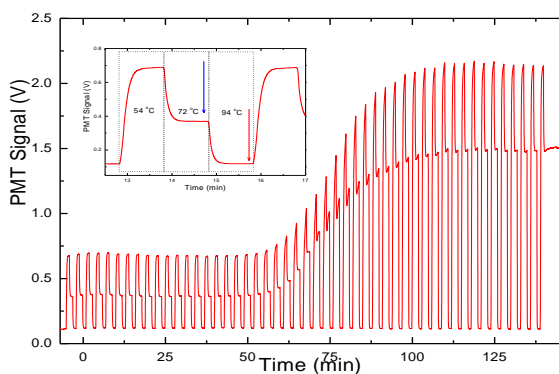


FIGURE 18 PCR AMPLIFICATION CURVE USING CONTINUOUS FLUORESCENCE MONITORING AND (INSET) SINGLE PCR STEP.

VRC with sample of a volume of a few  $\mu\text{L}$  covered with oil was illuminated via blue filter by metal halide light source using

upright microscope with long working distance objective lens. Emitted fluorescence collected by the same lens after passing through green filter interacted with a photomultiplier tube module (PMT) and its output voltage was recorded by an oscilloscope (Figure 18).<sup>21</sup> PCR protocol consisted of three steps: denaturation, annealing and extension at temperature of  $\approx 55 \text{ }^\circ\text{C}$ ,  $\approx 72 \text{ }^\circ\text{C}$  and  $\approx 94 \text{ }^\circ\text{C}$ , respectively. Each step duration was  $\approx 60 \text{ s}$  to make sure that the PCR will indeed be completed. Heating from temperature of  $\approx 72 \text{ }^\circ\text{C}$  to  $\approx 94 \text{ }^\circ\text{C}$  took  $\approx 0.5 \text{ s}$  and cooling from temperature of  $\approx 94 \text{ }^\circ\text{C}$  to  $\approx 55 \text{ }^\circ\text{C}$  lasted  $\approx 2 \text{ s}$ , corresponding heating rate of  $\approx 40 \text{ K}\cdot\text{s}^{-1}$  and cooling rate of  $\approx -20 \text{ K}\cdot\text{s}^{-1}$ .

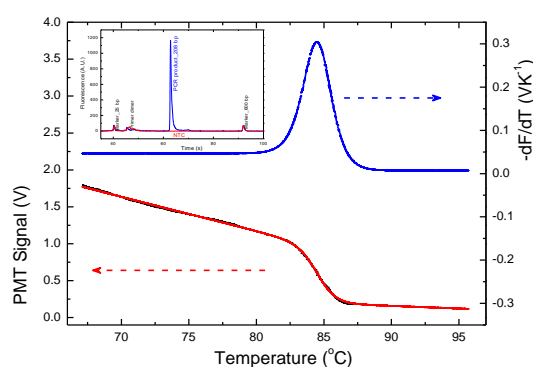


FIGURE 19 MELTING CURVE ANALYSIS (MCA) AND (INSET) CE ANALYSIS OF THE PCR PRODUCT.



Once the PCR was completed we immediately performed melting curve analysis/ (MCA) (Figure 19) and out of the PCR also capillary electrophoresis to make sure that the PCR amplification is specific and we did not create unwanted products, such as primer-dimer formation. Here we demonstrated for the first time that the PCR can be performed at silicon chip to take advantage of its excellent thermal properties. In the same time the chip was separated from the DNA template, it did not get contaminated and with new glass cover slip the chip was ready to be used again.

#### 2.1.4 NANO PCR SYSTEM

The previous system was simplified and we also lowered volume of the VRC (Figure 20). These changes allowed us to shorten a single PCR cycle to  $\approx 8.5$  s corresponding to perform 40 PCR cycles in  $\approx 340$  s.<sup>22</sup> The system in principle stayed the same.

Heater was again made by a patterned thin film gold integrated with micromachined silicon. This time the double donut shape was abandoned and we used only a single donut configuration. Due to this simplification as well as increasing the power supply voltage we were able to achieve a system with time constant of  $\approx 0.27$  s, heating rate of  $\approx 175$  K $\cdot$ s<sup>-1</sup> and cooling rate of  $\approx -125$  K $\cdot$ s<sup>-1</sup>.



FIGURE 20 MINIATURIZED VERSION OF THE MICRO PCR SYSTEM, SO CALLED NANO PCR WITH VCRS WITH SAMPLE WITH VOLUME OF 100 nL.

As with the “large” PCR system we pipetted the sample at the glass surface and covered with oil.

Here we used sample with volume of  $\approx 100$  nL and oil with volume of  $\approx 600$  nL (Figure 21). We found that the PCR ultimate speed is limited by the heat transfer between the heater and the sample through the glass and sample surrounding oil which took  $\approx 1.5$  s. Once the denaturation was shortened below  $\approx 1.5$  s the PCR amplification efficiency was dramatically lowered. Instead of a SYBR Green I we also

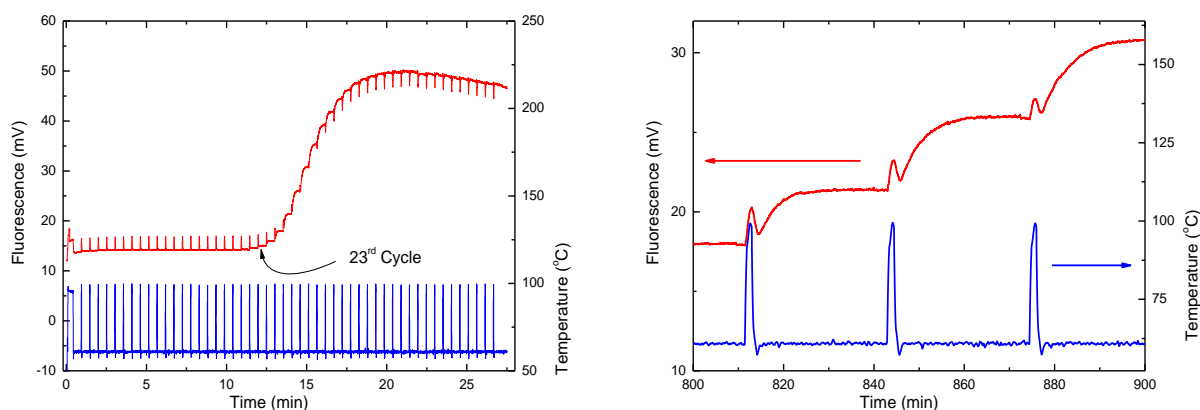


FIGURE 21 CONTINUOUS FLUORESCENCE MONITORING USING “NANO PCR” SYSTEM

used so called TaqMan chemistry<sup>23</sup> with 6-carboxyfluorescein (FAM) probe using only two temperature steps protocol.

We mixed solution for real-time PCR using TaqMan Fast Universal PCR Master Mix 2 (#4352042, Applied Biosystems, Inc.),  $\approx 0.5 \mu\text{l}$  Taqman Assays-by-Design (Applied Biosystems, Inc.) containing oligonucleotides and FAM probe for cDNA of green fluorescent protein (GFP): forward primer 5'-CACATGAAGCAGCACGACTT-3'; reverse primer 5'-CGTCGTCCTTGAAGAAGATGGT-3', probe 5'-FAM-CATGCCCCGAAGGCTAC-BHQ-1-3', and  $\approx 2 \mu\text{l}$  cDNA prepared by reverse transcription from transgenic gene GFAP-GFP. Length of the PCR amplicon was 82 bp.

This system performed very well and it was also exceptionally fast due to protocol simplification to two temperature steps, only denaturation and annealing/extension. We empirically found that the shortest time required for complete denaturation was  $\approx 1.5$  s. It was at that point of time limiting factor. Nevertheless this PCR was considered at that point of time as one of the fastest in the world, at least from heating and cooling rate point of views.<sup>24</sup>

Next natural step was performing RT-PCR in a VRC format. Therefore we prepared a single step RT-PCR master mix supplied by Roche Inc. for their LightCycler 1.5 system. It was a good choice as the PCR in the LightCycler was performed in glass capillary tubes and the master mix for it already contained optimized concentration of BSA. We chose artificially prepared RNA of an avian influenza virus H1N5 as at that time the avian influenza was a hot topic. Later on it was another type of influenza such as H1N3 swine flu, H7N9 avian flu and also Ebola virus. Unfortunately, this has nothing to do with science, the system we prepared had no preference what kind of DNA or RNA to amplify. It should process any type of RNA, regardless of its origin. Nevertheless for publication purposes, one has to create an interesting story and we learnt rather quickly, that current potential threat to human kind “sells” any work much better than the generic RNA or DNA.

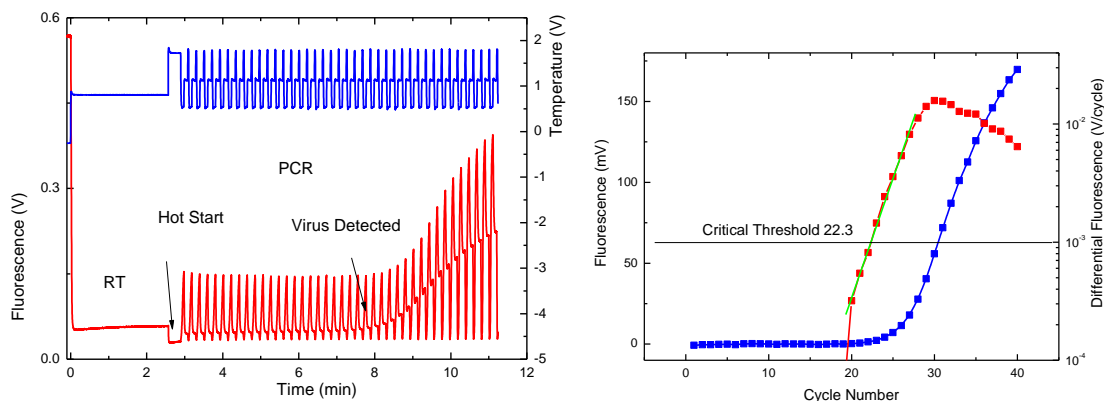


FIGURE 22 RT-PCR RNA OF AVIAN INFLUENZA VIRUS H5N1 AND EXTRACTED AMPLIFICATION CURVE PCR.



We tested an ultimate speed of the RT-PCR (Figure 22). The reverse transcription was conducted at  $\approx 61$  °C for  $\approx 2$  min followed by a hot start at  $\approx 95$  °C for  $\approx 30$  s. Hot start step had two functions. First it destroyed reverse transcriptase enzyme and also activated second enzyme polymerase. Subsequently we ran 40 cycles of the PCR each step consisting of three temperature sequences, denaturation, annealing and extension at usual temperatures of  $\approx 93$  °C,  $\approx 56$  °C and  $\approx 72$  °C. Single PCR step was done in  $\approx 14.5$  s. After completion of the PCR we also conducted MCA. With volume of  $\approx 200$  nL sample covered with  $\approx 600$  nL of M5904 mineral oil we were able to perform single PCR cycle in  $\approx 14.5$  s. Entire RT-PCR was achieved in less than 12 min.

Electrical and thermal parameters of both microPCR and nanoPCR are listed in table below:

Parameters	microPCR	nanoPCR
Sensor resistance (@ 25 °C)	320 $\Omega$	427 $\Omega$
Heater resistance (@ 25 °C)	110 $\Omega$	141 $\Omega$
Temperature response of the sensing system	11 mV/K (DC)	30 mV/K (AC)
Heat conductance	4.4 mW/K	0.42 mW/K
Heat capacitance	6.6 mJ/K	1.5 mJ/K
Thermal time constant	1.74 s	0.28 s
Heating rate from 60 °C to 95 °C	50 K/s	175 K/s
Cooling rate from 95 °C to 60 °C	-30 K/s	-125 K/s

### 2.1.5 INTEGRATED OPTICAL SYSTEM

Both previously described PCR systems required external microscope to monitor fluorescence. It was obviously only a temporary solution as fluorescent microscope was an expensive, bulky and delicate tool absolutely unsuitable for portable applications. Also it was highly disproportional, the PCR system occupied a volume of a few cm<sup>3</sup> with weight of 30 – 50 g and the microscope was at least 20  $\times$  bigger and 100  $\times$  heavier (Figure 23). It needed optics, sturdy body, and light source such as metal halide and a fluorescent system consisting of 3 optical filters, such as excitation, dichroic beam splitter and detection, PMT with power supply and recording system. We decided to develop a system with comparable parameters of a fluorescent microscope but small enough to be integrated into the PCR system for POC applications.

There were small systems optical systems commercially available and we decided to get inspired by them. We opened the DVD unit and looked at its pick-up head and its optics. In principal it had most features we also needed. It had light source, first filter, beam splitter (in fact two), focusing optics, second filter and light sensor. There were also some other components we did not intend to use, such as coil for system deflection to follow the track at recording media, flying head system to keep the distance between lens and track constant and a few more. We collected suitable elements, designed



FIGURE 23 FLUORESCENT MICROSCOPE USED FOR OUR WORK WITH PCR SYSTEM UNDERNEATH IT.

optical housing according to sizes of optical element and put everything together.<sup>25</sup> Entire system except the housing was made based on off-the-shelf elements. Focusing lens was model 354330-A supplied by Thorlabs, Inc. with diameter of  $\approx 6.35$  mm and numerical aperture of  $\approx 0.68$ . Other components had similar sizes. Instead of original red laser used in DVD we employed a turquoise color LED with principal emission of  $\approx 490$  nm. The diode was rather difficult to be obtained with high optical power output. There is very few manufacturers of this model as 490 nm is quite unpleasant looking blue-green color. Nevertheless its principal emission wavelength was favorable to induce fluorescence from fluorescein isothiocyanate (FITC) type system. As filter

set we purchased

47002 model from Chroma Optical, Inc. This filter set is multilayer interference type with some 150 layers. It has an exceptionally sharp cut-off, transparency  $\approx 0.98$  and light suppression out of transparent region better than  $\approx 10^6$ . We used a conventional silicon photodiode BPW21 made by Siemens with luminous detection area of  $\approx 7.4$  mm<sup>2</sup>. We also built-in transconductance amplifier to minimize ambient noise. It was based on an ultra-low noise diFET operation amplifier OPA 129 made by Texas Instruments. Entire optical housing has size of  $\approx 20$  mm  $\times$  20 mm  $\times$  10 mm (Figure 24 and Figure 25).

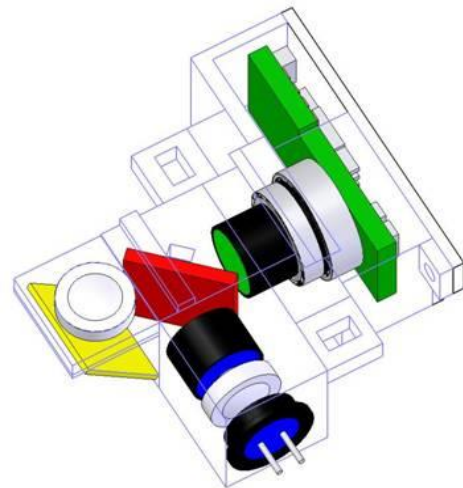


FIGURE 24 CAD DRAWING OF MINIATURIZED FLUORESCENT SYSTEM.

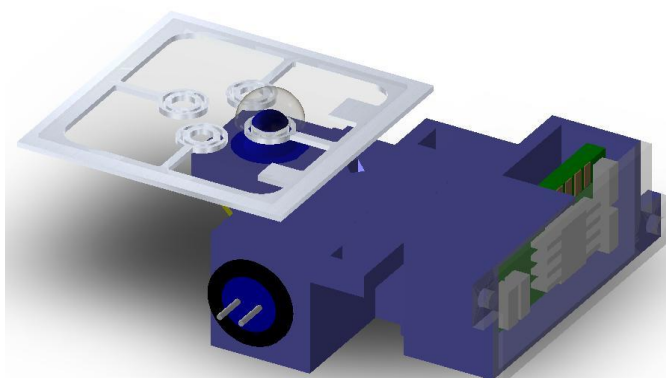


FIGURE 25 ENTIRE VIEW (CAD DRAWING) AT THE FLUORESCENT OPTICAL SYSTEM PLACED UNDER THE PCR CHIP WITH VRC

We found very quickly that the fluorescent signal amplitude from the system is insufficient for any meaningful work even with high magnification factor we used in transconductance amplifier system. The system was also very sensitive to ambient light and we had to operate in total darkness or inside a black box making it non practical.

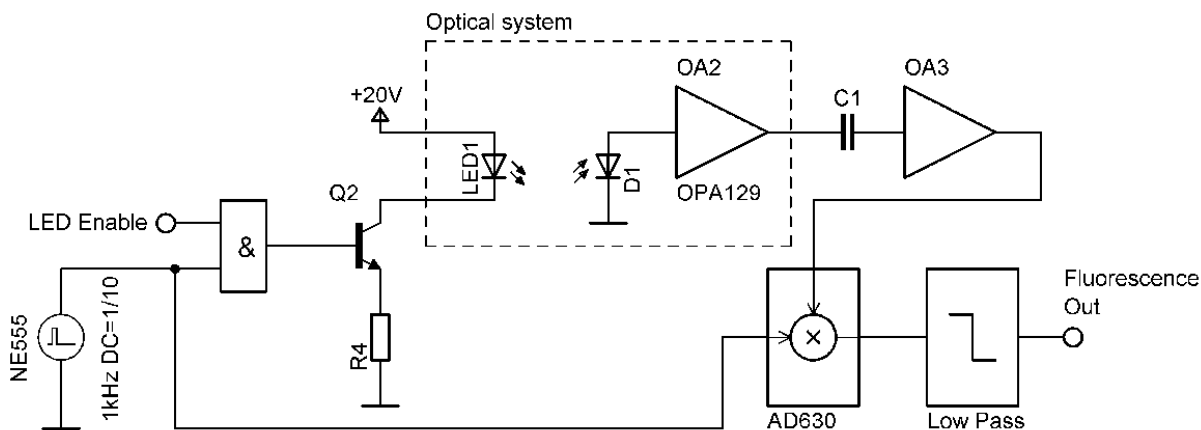


FIGURE 26 ELECTRONIC SCHEMATIC OF OPTICAL DETECTION SYSTEM WITH LOCK-IN AMPLIFIER.

Therefore we added an electrical modulator for the LED and a demodulator and a low pass filter to process the photodiode output signal. This system is called a lock-in amplifier and in principal it was very similar to the one we use for temperature measurement (Figure 26). It worked as extremely narrow bandwidth amplifier/filter. Only the signal with correct frequency the system was “locked to” could pass further. The lock-in amplifier typically improves the signal to noise ratio by factor between  $10^3$  and  $10^7$ . Light in our laboratory was either daylight, in principle DC light source, or came from fluorescent tubes, typically with frequency of 50 Hz. Therefore we carefully chose odd lock-in amplifier frequency to make sure that it is not a higher harmonics of 50 Hz. Typically we operated the lock-in amplifier at a frequency slightly above 1 kHz. The optical system was calibrated and we determined that minimum concentration of fluorescein we could detect was 1.96 nM. We also demonstrated that we could perform melting curve analysis (MCA) showing that the system’s sensitivity should be sufficient to perform real-time PCR.

#### 2.1.6 COMPLETE SYSTEM WITH SAMPLE PREPARATION I, DETECTION OF RNA OF H5N1 AVIAN INFLUENZA VIRUS

World health organization (WHO) assumes that the time frame to discover and quarantine pathogen outbreak is about 20 days. If that is not done the disease outbreak can get out of control and became pandemic. Disease discovery in developed countries as well as large cities in developing countries is relatively simple task. It rural areas in countries with limited economical resources it is rather difficult if not practically impossible. Having small, economical and easy to use infectious disease diagnostic systems is then absolutely essential to limit chance of pandemic.

In previous sections I showed bits and pieces of a real-time PCR system we were developing. Even with all those parts integrated together forming small real-time PCR system it is still not sufficient for practical disease diagnoses. Real-time PCR can detect presence of a purified RNA or DNA template in buffer solution. Real sample such as saliva, blood etc. contains genetic material inside cells or in viruses plus also PCR inhibitors. The virus (cell) has to be opened, RNA (DNA) released and PCR inhibitors

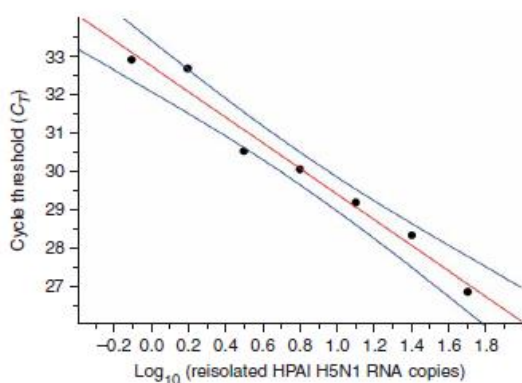


FIGURE 27 NORMALIZATION CURVE OF RT-PCR USING RNA OF H5N1 AVIAN INFLUENZA VIRUS.

removed. The virus (cell) opening is called lysis and it can be enzymatic, chemical or thermal. The sample has to be processed in reasonable quantity to make sure that even if the virus is presented in small quantity the system is able to diagnose its presence and avoid “false negative” result. Typical volume of sample to process is  $\approx 140 \mu\text{L}$ , which is too large for being processed at the glass surface.

The entire process was again performed at the highly hydrophobic glass surface with a set of VRCs having different functions for PCR such as RNA lysis, binding RNA to the surface of  $\text{SiO}_2$ , debris removal and RNA purification and finally performing real-time RT-PCR. In the first VRC we incubated the RNA at the  $\text{SiO}_2$  shell surface of super paramagnetic particles. Using strong magnet we moved the particles from VRC to VRC to perform entire process sequence.<sup>26</sup>

The entire process was again performed at the highly hydrophobic glass surface with a set of

The sample of  $40 \mu\text{L}$  of blood was spiked with known number of copies of RNA of avian influenza H5N1 virus and performed sequence of all steps described above to “discover” the RNA presence. Entire sequence lasted only  $\approx 28$  min. It started with pre-concentration of RNA when we were able to lower sample volume by factor of 500 without losing RNAs from the sample. We demonstrated that our system was as sensitive as the commercial one. We even achieved better performance as it was  $4.4 \times$  faster. The system was estimated to be at least  $200 \times$  cheaper. The RNA detection efficiency was  $\approx 99\%$  and we were able to demonstrate that the system is capable of detecting single molecule of RNA (Figure 27).

#### 2.1.7 COMPLETE SYSTEM WITH SAMPLE PREPARATION I, DETECTION OF RNA OF SARS VIRUS

We also prepared system to detect SARS virus. In fact we did not really detect the actual SARS virus, but its RNA transfected into other cells and performing entire process using harmless material. It was impossible to work with real virus for safety as well as formal and other reasons. Ability to work with the SARS virus requires laboratory equipped based on standard for biosafety hazard level 3 or 4 which we did not have. Therefore, we used cell from cell-line THP-1 transfected with GFP. We spiked blood with those cells, isolated them, pre-concentrated  $100 \times$ , purified, opened cell membrane (performed lysis) to release RNA and conducted real-time RT-PCR. Entire process took only  $\approx 17$  min. Here we used space domain PCR. We used 3 – 4 heaters kept at constant temperature and with magnetic force we moved sample between zones with different temperature performing the RT-PCR.<sup>27</sup>

## 2.2 REAL-TIME PCR OF 1<sup>ST</sup> GENERATION

In previous chapters I described development of very fast PCR as well as small fluorescent optical detection system. We combined both together including single chip controller and created the first generation of miniature real-time PCR (Figure 28). It had built-in temperature control system for fluorescence monitoring, graphical LCD control and generation of all required voltages from a single

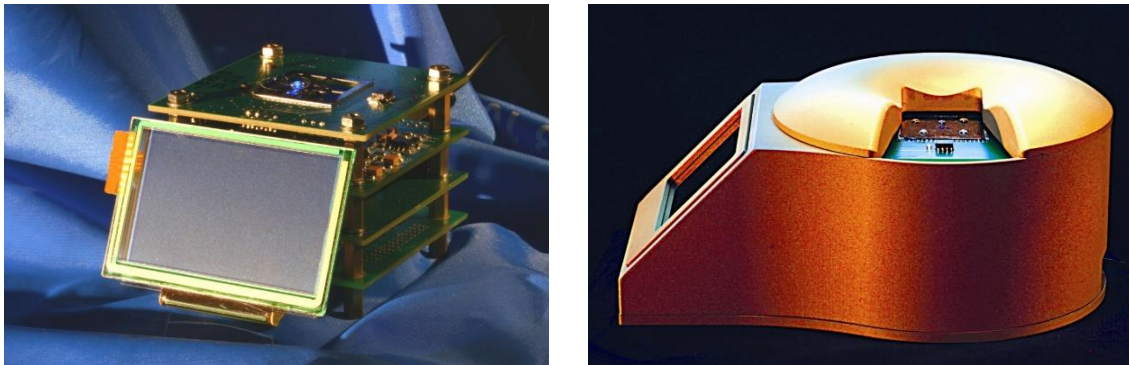


FIGURE 28 PHOTOGRAPH OF A REAL-TIME PCR SYSTEM OF FIRST GENERATION. (LEFT) ONCE THE HOUSING IS REMOVED ONE CAN SEE INDIVIDUAL PCBs WITH ELECTRONICS. (RIGHT) ENTIRE SYSTEM IN PROTECTIVE COVER AFTER TREATED BY ANODIC OXIDATION.

voltage power supply of 12 V.<sup>28</sup> The optical system was quite small but even with its small size we were able to integrate only a single optical unit. Due to that limitation we were able to process only a single sample a time (Figure 28). Nevertheless we were able to demonstrate detection of RNA from a segment of H5N1 avian influenza virus using single step real-time RT-PCR. We employed again LightCycler® RNA Master SYBR Green I one-step RT-PCR kit produced by Roche, Inc. (Figure 29). Specific oligonucleotides were supplied by our collaborators from Genome Institute of Singapore (GIS), A\*STAR, Singapore. Forward primer was: 5'-TGCATACAAA TGTCAAGAAAGG-3' and reverse primer was: 5'-GGGTG TATATTGTGGAATGGCAT-3'.

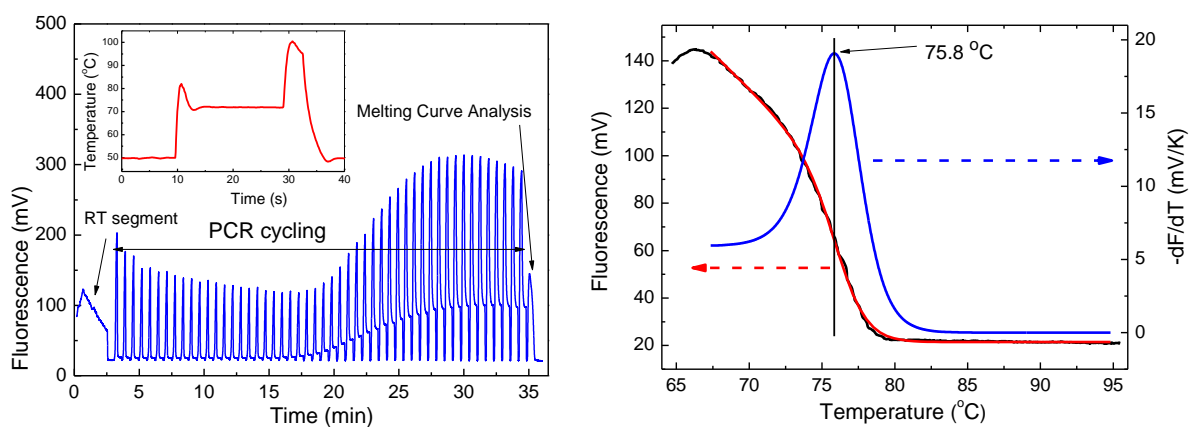


FIGURE 29 (LEFT) DETECTION OF H5N1 AVIAN INFLUENZA RNA USING REAL-TIME PCR SYSTEM OF 1<sup>ST</sup> GENERATION. (RIGHT) MELTING CURVE ANALYSIS (MCA).



Entire process took  $\approx 35$  min including reverse transcription and melting curve analysis. Expected melting temperature of amplicon was  $\approx 76$  °C and we measured  $\approx 75.8$  °C, which is near perfect match. That confirmed that we did achieve specific cDNA replication and that we did not have different unwanted PCR.

### 2.3 REAL-TIME PCR OF 2<sup>ND</sup> GENERATION (UNIVERSAL LOC SYSTEM)

While we compared our real-time PCR and other LOC system we found that there is many similarities. Temperature regulation is very common, regardless it is for PCR in range between  $\approx 50$  °C and  $\approx 95$  °C or for cell culturing at  $\approx 37$  °C. Also there is some kind of product detection, either optical such as fluorescence, reflection, absorption or electrical using electrochemical or conductometric sensors. Often here is sample manipulation, sometimes high voltage power supply is required for compound separation and practically we have to always display results.

We developed entire family of LOC systems based on a single universal platform.<sup>29</sup> It was portable application-specific lab-on-a-chip (ASLOC) which was easy to reconfigure for wide variety of LOC applications. The top three PCBs were application specific while all other boards were the same. The reconfiguration meant to replace top PCBs with new ones and upload specific software for that particular application to process the signals (Figure 30). The system was controlled by a single chip controller and the embedded program could be uploaded with USB interface.

The core of the system was 4-channel lock-in amplifier for detection of LOC products (Figure 31). It contained four programmable pulse generators each of them operating at different frequency. Via bipolar junction transistors we generated current pulses which powered directly LEDs or via

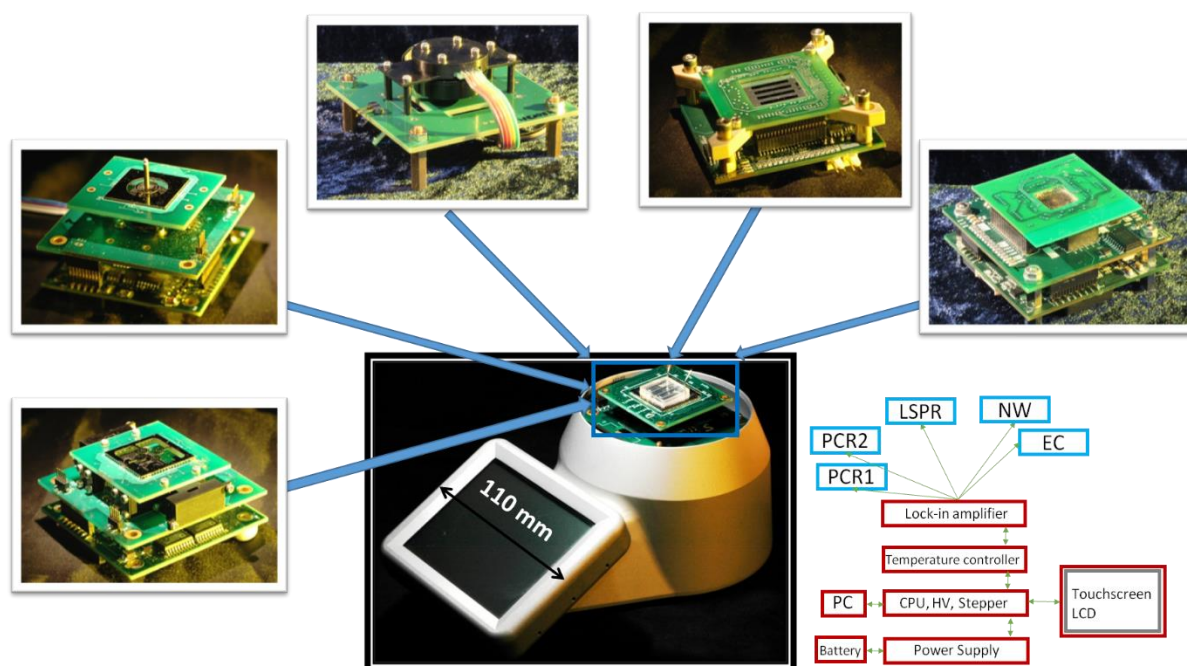
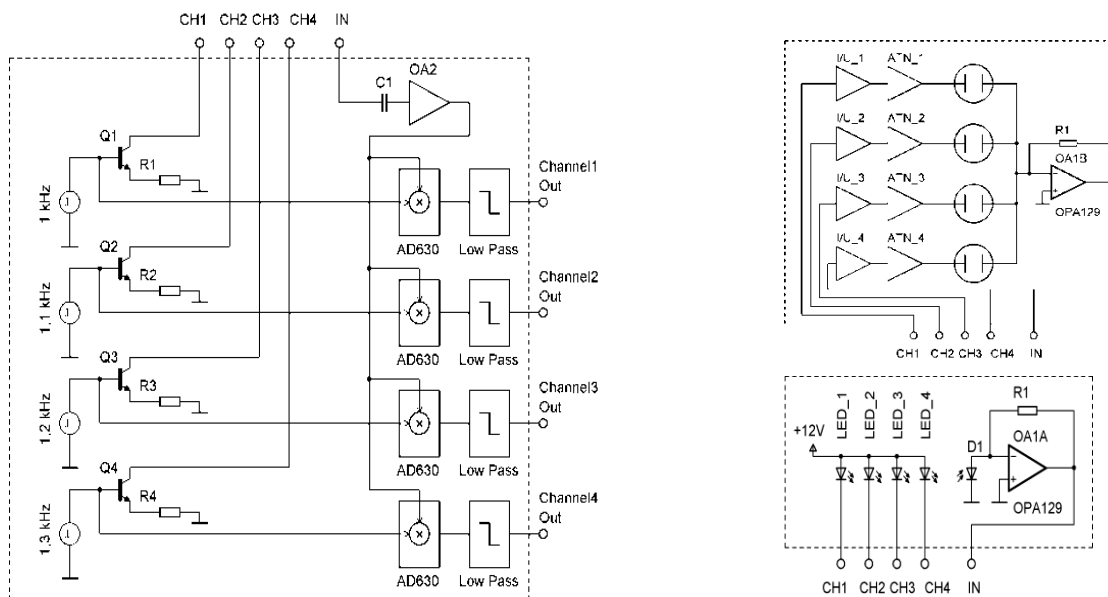


FIGURE 30 MODULAR LOC SYSTEM OF SECOND GENERATION



**FIGURE 31 (LEFT) CORE OF THE LOC SYSTEM OF SECOND GENERATION. FOUR SIGNAL GENERATORS WITH DIFFERENT FREQUENCIES. (RIGHT TOP) SYSTEM TO MEASURE ELECTRICAL CONDUCTIVITY OF SILICON NANOWIRES OR TO WORK WITH ELECTROCHEMICAL CELLS. (RIGHT BOTTOM) OPTICAL DETECTION SYSTEM.**

current/voltage converters and attenuators we biased nanowires or electrochemical cells (pseudo reference electrodes). Composite voltage from transconductance amplifier was further amplified after DC offset removal and separate by 4 demodulators into individual compounds based on modulating frequencies.

Each channel had in fact two signal generators (based on a microcontroller), one to interrogate the LEDs (NW, electrochemical cells etc.) and a second one for demodulation. Both operated with identical frequency and duty cycle but there was controllable phase shift between them. We found that the signal processed via LED, fluorescence, photodiode is delayed by approximately 28  $\mu$ s compare to the signal from generator fed directly into the demodulator. Compensating the delay using second signal generator improve the signal efficiency by  $\approx 30\%$ . All those three parameters, frequency, duty cycle and delay of second signal generator were remotely controlled by external PC using RS 232 protocol.

The processed signals were either loaded to oscilloscope and displayed by it during development phase or processed by embedded software and displayed at its LCD.

Optical sensing properties of this LOC were demonstrated with two channel real-time PCR in time domain as well as single channel in space domain. We also demonstrated with modified optical head to detect effects of localized surface plasmon resonance (LSPR) on a nanostructured gold surface. This system's capability to monitor biosensors based on change of electrical parameters was also tested using an array of nanowires and electrochemical sensors. Here we added an analog multiplexer (switch)  $1 \times 16$  into each channel thus expanding its capability from 4 to 64 sensors.

### 2.3.1 LSPR SYSTEM

The first finished LOC system using the 2<sup>nd</sup> generation platform was based on light reflection from an LSPR chip.<sup>30</sup> The chip was illuminated by 4 LEDs each of them with different color and we were able to monitor in a real-time surface properties of that chip. We demonstrated that the different analytic composition changing LSPR surface optical absorption can be monitored by the system. (Figure 32).



FIGURE 32 LSPR SYSTEM.

### 2.3.2 NW SYSTEM

That time I worked in IME, A\*STAR, Singapore and we had large program for application of silicon nanowires. One of our focused areas was bio applications such as DNA and protein detection. Researcher claimed that the nanowires and other label free systems are great for detection of practically any bio substance. I have

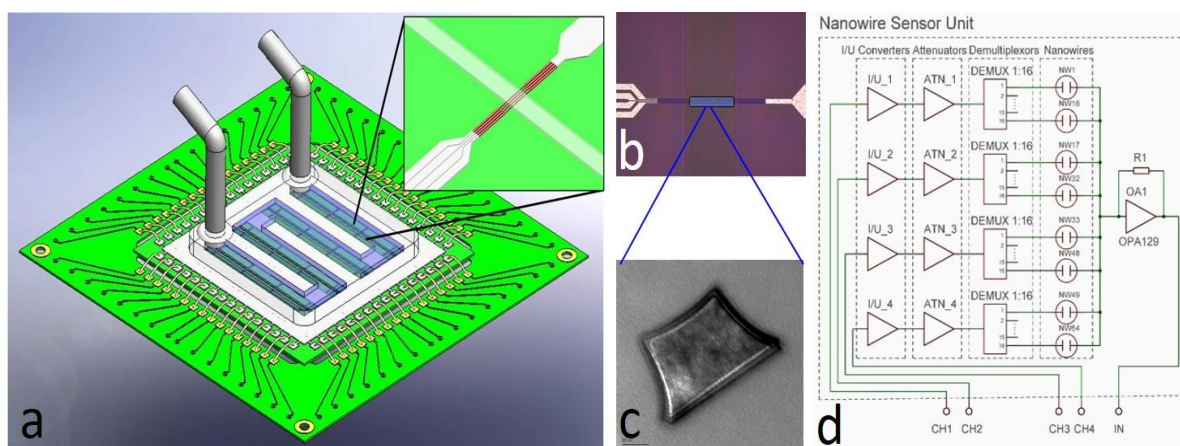


FIGURE 33 CAD IMAGE OF A SYSTEM WITH 64 NANOWIRES (NW).

my doubt that the label-free technique will ever be able to compete with the PCR as the PCR is an excellent detecting technique for both, DNA as well as RNA. Detection of proteins is another story.

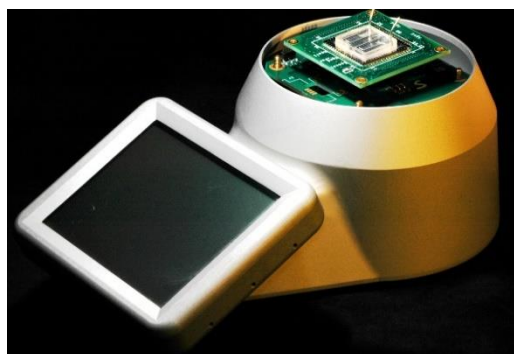


FIGURE 34 PHOTOGRAPH OF LOC SYSTEM OF 2<sup>ND</sup> GENERATION WITH CHIP HAVING 64 NANOWIRES AND MICROFLUIDIC CHIP MADE OF PDMS.

There the gold standard is enzyme-linked immunosorbent assay (ELISA) which requires two specific antibody-antigen reactions. It is rather slow process and researchers are looking for an alternative solutions. Nanowire-based systems could be one of them.

The original system to test 4 samples a time was expanded by adding two double analog switches 1 out of 16 (Figure 33) and thus increased number of measured channels (sensors) to 64.<sup>31</sup> We also designed new chip with 64 NWs in configuration suitable for this testing. We



had to cluster the nanowires into group of 4 (Figure 34). The system was tested using solute with different pH.

## 2.4 REAL-TIME PCR OF 3<sup>RD</sup> GENERATION

### 2.4.1 TECHNICAL CONCEPT

We soon realized that the entire concept of LOC of 2<sup>nd</sup> generation was not very successful. Having a universal LOC which is capable of performing practically any LOC method does not make much sense. In a laboratory focused on electrochemical methods is unlikely to use PCR, nanowires or vice versa. Thus the concept of modular LOC does not offer anything extra and the system is rather complicated due to its versatility. Our main interest was still the real-time PCR and the LOC of 2<sup>nd</sup> generation was capable of performing only 2 reactions a time and required 6 optical filters. The concept was just too expensive and 2 PCRs a time were not sufficient for practical applications. We thus set the requirements of a new system of 3<sup>rd</sup> generation:

- Performing concurrently 4 real-time PCRs
- Negative and positive control plus two samples
- Palm size
- Capable of detecting RNA, i.e. performing the RT-PCR

We took advantage of our knowledge gained in the course of previous work and developed a new real-time PCR system (Figure 35). As far as I know, with its dimensions of  $\approx 100 \text{ mm} \times \approx 60 \text{ mm} \times \approx 33 \text{ mm}$  and weight of  $\approx 75 \text{ g}$ <sup>32</sup> it is without practically any competition the smallest real-time PCR in the world.<sup>33</sup> We again used the concept of VRCs placed on a disposable glass above the micromachined silicon chip. In comparison with previous systems we simplified the optics as well as the electronics. The four VRCs required only 5 optical filters in total instead of expected 12. Two systems shared the same excitation filter and dichroic mirror and there was only a single emission filter for all four systems (Figure 36). There was only one temperature controller as we used serial-parallel combination of all four heaters as well as four sensors. The electronic system to detect the fluorescence was also only

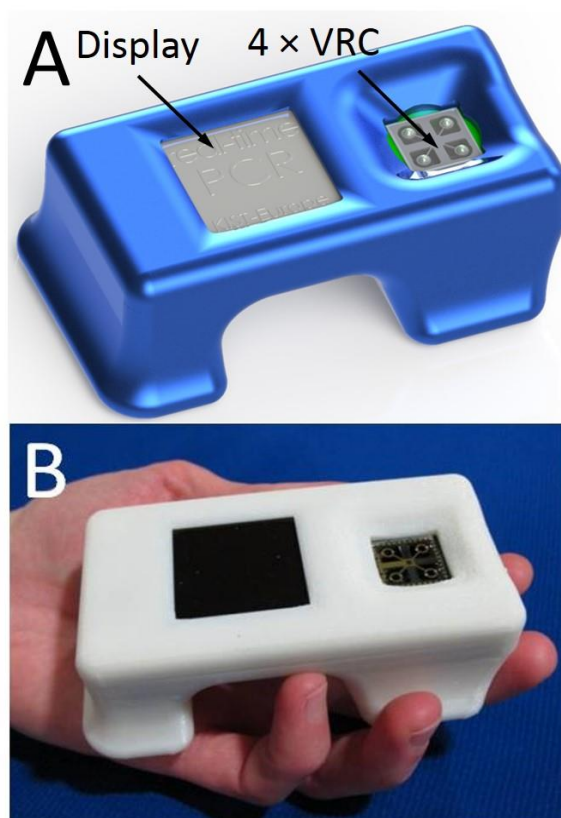


FIGURE 35 REAL-TIME PCR OF 3<sup>RD</sup> GENERATION. (A) CAD DRAWING AND (B) FABRICATED SYSTEM.

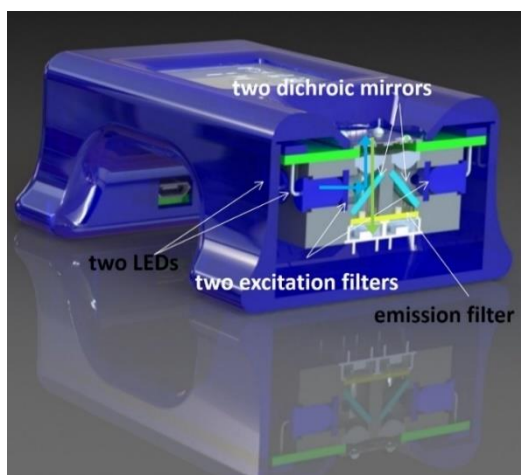


FIGURE 36 CROSS-SECTION OF OPTICAL PART OF THE SYSTEM SHOWING LIGHT PATH.

Only at the end of extension step, the closed feedback loop used to control temperature was disconnected for last  $\approx 2$  seconds. We used an average duty cycle of the PWM measured during “controlled part” of the extension step and the lock-in amplifier was utilized for fluorescence measurement, half a second per each VRC. We used this system to detect 4 samples containing cDNA of an avian influenza H7N9 virus each with volume of  $\approx 200$  nL. One VRC was used for negative control, one for positive and two were emulating actual samples (Figure 37). We also performed a standard PCR curve showing that the system was capable of detecting a single cDNA copy with an efficiency of  $(0.91 \pm 0.05)$  (mean  $\pm$  standard error).

#### 2.4.2 APPLICATIONS

We show the utilization of a recently developed palm-sized real-time polymerase chain reaction (PCR) device to detect RNA of an Ebola virus using single-step reverse transcription PCR (RT-PCR). The device was shown to concurrently perform four PCRs each with a volume of  $\approx 100$  nL: one positive control with both Ebola and GAPDH RNA, one negative control. The last two positions were used to measure the GAPDH and the Ebola content of a sample. The comparison of critical thresholds from the two samples provided relative quantification. The entire process, which consisted of reverse transcription, PCR amplification, and melting curve analysis, was conducted in less than 37 minutes. The next step will be integration with a sample preparation unit to form an integrated sample-to-answer

one. All 4 photodiodes were connected to the same lock-in amplifier and only the active one was selected by powering its LED and only one LED was powered a time. The fluorescence amplitude was measured only once during each cycle at the end of an extension step. During RT section of the protocol the fluorescence was not measured at all. So did we really need a dedicated system for fluorescence measurement as the same one was used to measure the PCR temperature? The single lock-in amplifier was then used for both, temperature measurement as well as fluorescence signal processing. The lock-in was normally used to monitor temperature.

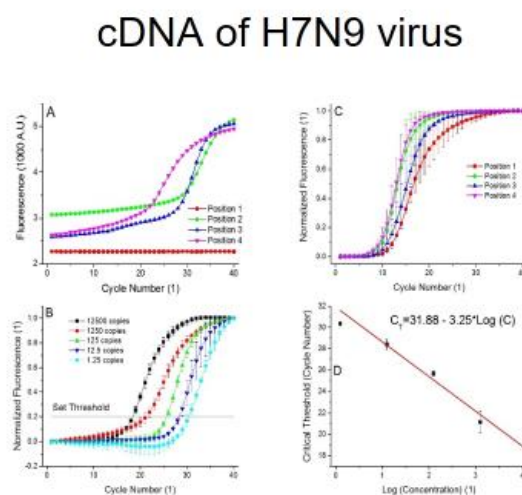


FIGURE 37 RESULTS FROM THE REAL-TIME PCR SYSTEM OF 3<sup>RD</sup> GENERATION SHOWING DETECTION OF cDNA OF AN AVIAN INFLUENZA VIRUS H7N9.

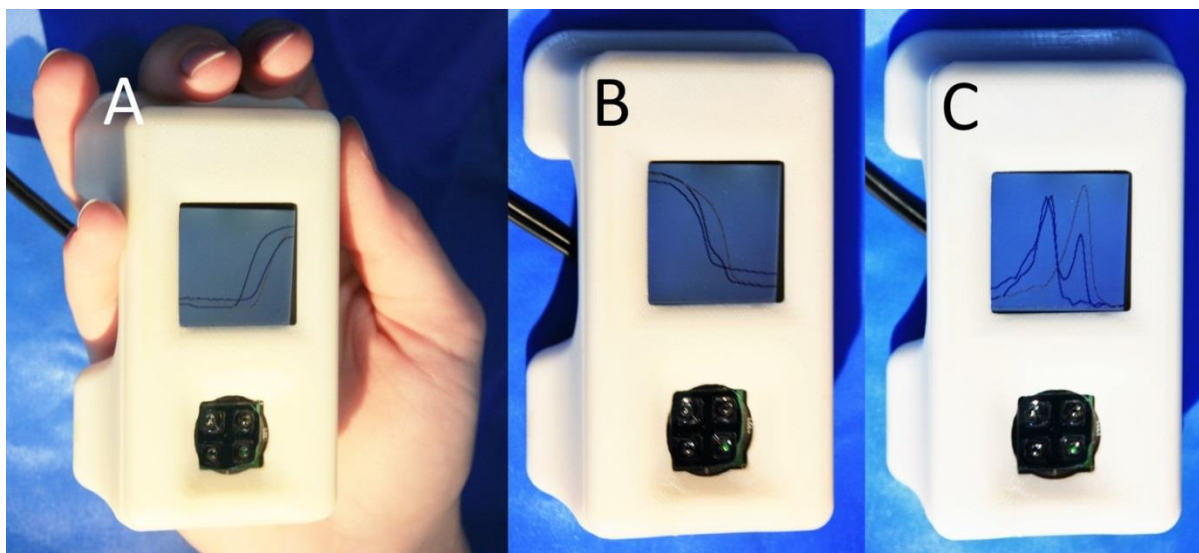


FIGURE 38 HAND HELD DEVICE OF 3<sup>RD</sup> GENERATION SHOWING DETECTION OF EBOLA VIRUS RNA. (A) REAL-TIME PCR RESULT (B) MELTING CURVE ANALYSIS AND (C) ITS DERIVATIVE.

system for point-of-care infectious disease diagnostics. The manuscript is currently under consideration in **XX** journal.<sup>34</sup>

## 2.5 OTHER RESULTS

In course of development of the LOC systems we also published other results related to our main effort. They are briefly described in this section.

### 2.5.1 CONTACTLESS TEMPERATURE MEASUREMENT

Temperature measurement inside system with small volume is always a challenge. Even miniature temperature sensor such as resistive temperature detector (RTD) has size of  $\approx 1 \times 2$  mm is far too large for microfluidic channels having the size in tens of  $\mu\text{m}$ . It has also to be connected to the electronic interface system by wires and heat flux through those wires can negatively affect the measurement. Besides that it is impossible to insert such a device inside the microchannel. Noncontact temperature measurement seems to be a good solution. Very well known is infrared sensing, either thermopile-based for non-contact temperature measurement or bolometer-based thermovision. These systems operate by absorption infrared radiation in wavelengths from  $8 \mu\text{m}$  to  $14 \mu\text{m}$ . There are two fundamental problems. These systems do not measure the temperature, but the amplitude of heat radiation, which is sensitive to surface properties such as its emissivity. Also conventional glass is transparent in visible range of electromagnetic radiation as well as in near IR band. Nevertheless it is opaque for medium IR wavelength from  $8 \mu\text{m}$  to  $14 \mu\text{m}$  making this system impossible to be used to determine temperature inside the microfluidic channels. A few years ago temperature sensitivity of the fluorescence amplitude of fluorescein was demonstrated.<sup>35</sup> It seems like a great technique, the fluid itself was the temperature sensing material. However, the problem lies in so called photobleaching effect making the precise temperature determination impossible. Depending on the pH fluorescence amplitude of fluorescein

decreased with time. We utilized knowledge of MCA using two different DNA amplicons, each with different melting temperature.<sup>36</sup> Amplitude of the fluorescence indeed decreased with time due to photobleaching effect, but the melting temperatures were shown to be time independent. We also demonstrated that the system can be used to determine heat transfer rate between heater and the sample inside the VRC.

### 2.5.2 SUPERHEATING

Accidentally we found that we were able to warm up the water-based sample inside the VRC to relatively high temperature without actual boiling. Is it known that liquid requires two conditions to be fulfilled to boil: achieving boiling temperature corresponding to surrounding pressure and presence of nucleation seeds. There are two different interfaces within the VRC, optical quality glass surface and interface between two immiscible liquids. None of them contained any scratches necessary for boiling.

#### 2.5.2.1 DNA RELEASE FROM SPORES

We heated up samples containing pores of *bacillus subtilis* to different temperatures between  $\approx 100$  °C and  $\approx 200$  °C for  $\approx 10$  s. We used two systems, capillary as well as the VRC. After exposure of the sample to nominal temperature we used real-time PCR to determine DNA of *bacillus subtilis* in the sample.<sup>37</sup> We found that temperature above  $\approx 120$  °C did destroy the spores but certain ratio of released DNA survived those harsh conditions of overheated water to be detected by real-time PCR method. The capillary-based system was easier to be used. We could achieve temperature up to  $\approx 240$  °C without boiling for more than half an hour and also  $\approx -12$  °C without water freezing.

#### 2.5.2.2 PHYSICS OF OVERHEATED VRC

We developed an ultrafast system capable of warming up at incredible heating rate of  $\approx 650$  °C/s. Once we collected experimental data we also modeled transitional behavior of the system using finite element analysis software (FEA) ANSYS. The simulation results were compared with temperature measurement from the droplet by monitoring fluorescence amplitude from fluorescein solution in the VRC as function of time. The model was simplified by replacing water and oil with solid matter with correct thermal properties of both, water and oil. We then experimentally found that real temperature inside the VRC rose faster than the one predicted by ANSYS.<sup>38</sup> It was probably due to fluid convection induced by non-uniform heating as we did observe using optical microscope that the sample moved quite violently once it was heat up to high temperature. This moving kept equalizing temperature inside the VRC. In contrary the ANSYS model assumed solid matter and heat was only transferred by heat flux.

#### 2.5.2.3 PEPTIDE HYDROLYSIS

We utilized the VRC with overheated water-based sample to peptide hydrolysis<sup>39</sup> just before sample analysis by mass spectroscopy. We were able to reach temperature up to  $\approx 240$  °C without boiling the sample. We heated ACTH1-10 and OVA257-264 peptides to different temperatures and investigated degrees of their decomposition. We were able to demonstrate that this technique can be used as first step of tandem mass spectroscopy.

### 2.5.3 PCR TECHNIQUE DEVELOPMENT

#### 2.5.3.1 MULTIPLEXING I

Sample during the PCR is heated up from annealing temperature (typically around  $\approx 56$  °C) to extension temperature (typically around  $\approx 72$  °C) and from extension to denaturation (typically around  $\approx 93$  °C). When the sample was warmed up to denaturation temperature the dsDNA molecule melted into two ssDNA molecules, which was the same process as the one used during melting curve analysis (MCA). In presence of intercalating dye such as Eva Green we performed continuous fluorescence and temperature monitoring obtaining two relationships for both, fluorescence and temperature as function of time:

$$F = f(t), T = f(t) \quad (8)$$

We were able to eliminate time from both equations (8) resulting in fluorescence as function of temperature for each cycle of PCR called a dynamic MCA. We analyzed all 40 PCR cycles thus performing multiple quantitative PCR using single fluorescent channel. The only requirements were the ability to perform continuous fluorescent monitoring, different melting temperature of each amplicon by at least 3 °C and small sample volume to limit internal sample temperature gradient during transition period. The “nano-PCR” under optical microscope did fulfill all requirements. We have demonstrated this method for multiple detection of cDNA of hemagglutinin (HA) a neuraminidase (NA) genes from avian influenza virus H7N9.<sup>40</sup> We would thus improve diagnoses precision of this dangerous virus as well as to determine the safety hazard as that one depends on the ratio of both genes.<sup>41</sup>

#### 2.5.3.2 MULTIPLEXING II

I mentioned several times that our real-time PCR was conducted typically with intercalater dye such as SYBR-Green I or Eva-Green. Once the sample with dsDNA warmed up above the DNA melting temperature, the fluorescence amplitude sharply diminished. The ultrafast PCR system was based on a FAM probe, where the dsDNA melting had no influence on the fluorescence amplitude. We combined two types of oligonucleotides, one pair specific to DNA 1 with FAM probe and the second pair specific to DNA 2 without. We then performed the real-time PCR in the presence of intercalater. Both amplicons contributed to fluorescence amplitude at  $\approx 72$  °C due to the intercalater binding into their dsDNA as well as the FAM probe from DNA 1. Once the sample temperature overcame the melting temperature of both amplicons, only the FAM probe contributed to the fluorescence signal. We then extracted two sets of curves, at the end of extension step and at the end of denaturation step. Only amplicon related to DNA 1 contributed to the second one, which we then subtracted from the composite signal at the extension step.<sup>42</sup>



## 2.5.4 PYROSEQUENCING

There is enormous interest in DNA structure and its sequence. Human genome project greatly increased this interest with results in development of various methods to determine the DNA sequence.<sup>43</sup> One of them is called pyrosequencing.<sup>44,45</sup>



FIGURE 40 A PHOTOGRAPH OF A GLASS WITH 4 VRCs CONTAINING NUCLEOTIDES A, C, G, AND T (WE USED COLOR INK FOR CONTRAST ENHANCEMENT) SURROUNDING THE VRC SERVING AS WASHING STATION TO WASH DNA AND REMOVE DEBRIS FROM PREVIOUS REACTION.

incorporated into the DNA strain and amplitude of emitted light shows how many nucleotides were incorporated. We again used microscope glass cover slip with hydrophobic surface coating using VRC configuration (Figure 40 and Figure 39).

We incubated ssDNA on superparamagnetic particles and using strong permanent magnet to move those particles from VRC to VRC. Emitted light was monitored by a photomultiplier tube. Particles had to be aligned with the PMT. It was more convenient to keep particles and PMT above each other while the stage holding the glass was moved.

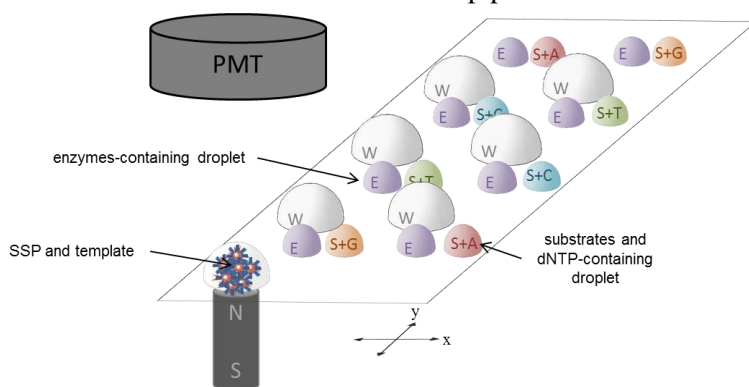


FIGURE 41 PRINCIPLE OF PYROSEQUENCING SYSTEM.

We demonstrated that there was a simple way to perform DNA pyrosequencing at the glass surface without necessity of purchasing large and expensive pyrosequencing tool. We only used light detector, hydrophobically coated glass, pipette and an ability to move the glass in controlled manner from place to place (Figure 42). Manuscript of this work is currently under review in Lab-on-a-Chip journal.<sup>46</sup>

This technique is based on an incorporation of nucleotide into a chain of a single stranded DNA. Nucleotide addition releases a molecule of PPi and triggers a sequence of biochemical reactions. As result there is adenosine triphosphate which in presence of luciferase and luciferin produces light (Figure 39). Light presence demonstrates that the reaction did occur and thus the nucleotide was

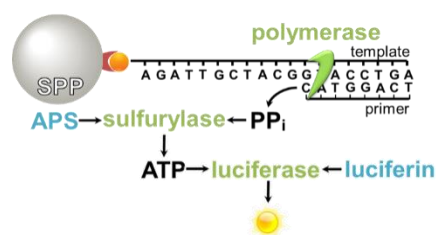


FIGURE 39 PYROSEQUENCING PRINCIPLE

the glass was moved. There was no need to move the PMT as the only reactions emitted light were conducted about the magnet.

We demonstrated that there was a simple way to perform DNA pyrosequencing at the glass surface without necessity of purchasing large and expensive

## 2.5.5 OTHER WORK IN MICROFLUIDICS

We studied generation of electrochemoluminescence at free metal platelets in solution.<sup>47</sup> Electrochemical reaction of tris(2,2'-bipyridyl) dichlororuthenium(II) hexahydrate [Ru(bpy)<sub>3</sub>]<sup>2+</sup> with

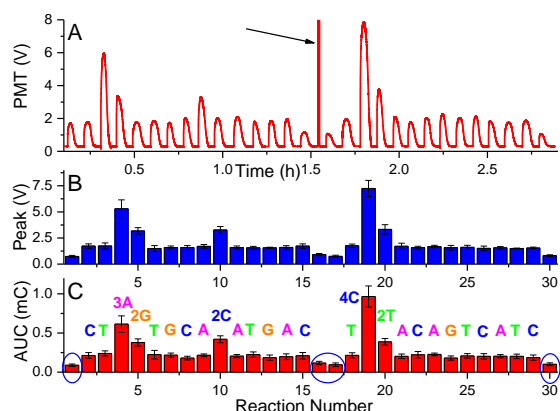


FIGURE 42 PYROGRAM (A) AND EXTRACTED AREA (B) AND PEAK VALUES (C).

co-reactant 2-(dibutylamino) ethanol DBAE resulted in emitting light. We applied a voltage across capillary inducing electrical field inside it. Electrical conductivity of metal platelets was much higher than the one of surrounding solution creating potential drops between platelets both ends and the solution, one side behaved as cathode and the other side as anode. The solution was oxidized at anode side of the platelets producing light without any electrical connection to an external power supply.

Another work I would like to mention was sugar chemistry to emulate cell walls.<sup>48</sup> Functionalized microbeads were bound to the microfluidic channels and greatly increased the surface-to-volume ratio of the system. Much greater number of biomolecules enhanced the sensitivity of biochemical analyses. We also used sugar chemistry to monitor circulating metastatic cells in a microfluidics assay for early cancer detection and monitoring cancer treatment efficiency.<sup>49</sup>

Two liquids entering the same microchannel from different directions flow parallel with each other without mixing due to small Reynolds number typical for microfluidics. Nevertheless the ions could be extracted from one fluid into the second one using electric field. We investigated membrane-free liquid-liquid-phase extraction using aqueous two phase systems.<sup>50</sup>

A system showing direct coupling of a free-flow isotachopheresis (FFITP) device with electrospray ionization mass spectrometry (ESI-MS) was recently published.<sup>51</sup> We presented the online coupling of a free-flow isotachopheresis (FFITP) device to an electrospray ionization mass spectrometer (ESI-MS) for continuous analysis without extensive sample preparation.

We study in vitro liver functions and liver cell specific responses to external stimuli with the problem to preserve the in vivo functions of primary hepatocytes. We used the biochip OrganoPlate<sup>TM</sup> (MIMETAS) that combined different advantages for the cultivation of hepatocytes in vitro: (1) the perfusion flow was achieved without a pump allowing easy handling and placement in the incubator; (2) the phase guides allowed plating of matrix-embedded cells in lanes adjacent to the perfusion flow without physical barrier; and (3) the matrix-embedding ensured indirect contact of the cells to the flow. In order to evaluate the applicability of this biochip for the study of hepatocyte's functions, Matrigel<sup>TM</sup>-embedded HepG2 cells were cultured over three weeks in this biochip. Chip-cultured cells

grew in spheroid-like structures and were characterized by the formation of bile canaliculi and a high viability over 14 days. Hepatocyte-specific physiology was achieved as determined by an increase in albumin production. Improved detoxification metabolism was demonstrated by strongly increased cytochrome P450 activity and urea production. Additionally, chip-cultured cells displayed increased sensitivity to acetaminophen. Altogether, the OrganoPlate seemed to be a very useful alternative for the cultivation of hepatocytes, as their behavior was strongly improved over 2D and static 3D cultures and the results were largely comparable and partly superior to the previous reports on biochip-cultured hepatocytes. As for the low technical needs, this platform has the appearance of being highly applicable for further studies of hepatocytes' responses to external stimuli and compared to a static Matrigel culture (3D) and a monolayer culture (2D).<sup>52</sup>

Finally we also used light guides for microfluidics applications but I consider this work rather marginal so the published papers are not attached here.<sup>53-57</sup>

#### 2.5.6 REVIEW

I would also like to mention our publication in prestigious journal of Nature Reviews Drug Discovery.<sup>58</sup> We discussed in details advantages of microfluidics systems for drug discovery as well as future trends in this field.

### 3. FUTURE WORK

Together with Dr. Bartošík from Recamo and Prof. Paleček from Biophysical Institute, both from Brno, Czech Republic, we are currently finishing an electrochemical system for the multiplexed detection of 4 different proteins or DNAs in 4 different samples. It is based on a LOC system of the second generation. The principle of measurement is very similar to the one we used for nanowire testing. The structure contains 64 sensors in an array configuration of 4 x 4. Each of them sensing area of the array contains 4 electrochemical system based on 2 electrode configuration (Figure 43). We have preliminary data (Figure 44) but due to technical difficulties, the chip has to be redesigned and fabricate once more. The working electrode has a donut shape with width of  $\approx 6 \mu\text{m}$  surrounded with reference/counter electrode with 20 $\times$  larger area than the one of the working electrode. Preliminary study showed that the working electrode has a microelectrode behavior. We observed a sigmoidal shape of the cyclic voltammogram typical for microelectrodes instead of a "classical shape" with oxidation and reduction peaks. Also the pulse method used for the measurement is a promising tool as it is capable of low current measurement. On the top of that the multiplexing method in LOC 2<sup>nd</sup> generation enables to measure up to 64 systems in short time period, always 4 systems a time.



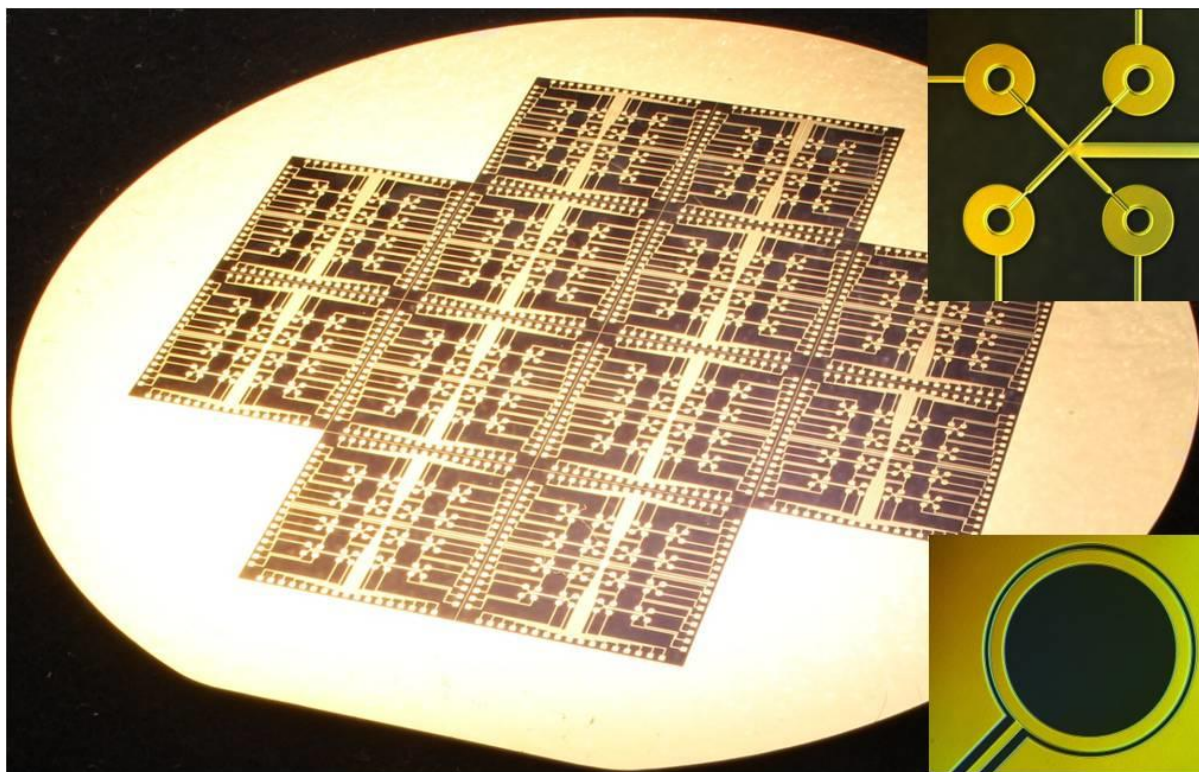


FIGURE 43 FABRICATED GLASS WAFER WITH DIAMETER OF 100 MM CONTAINING 12 CHIPS EACH WITH 64 ELECTROCHEMICAL SENSORS. (TOP RIGHT) DETAIL OF A SET OF 4 EC CELLS AND (BOTTOM RIGHT) A SINGLE WORKING ELECTRODE SURROUNDED BY A REFERENCE/COUNTER ELECTRODE.

We will also finish testing of a real-time PCR of third generation by detecting food pathogens, such as *Escherichia Coli* (*E. Coli*) bacteria serotype of O157:H7 producing Shiga toxin. It should work as we were able to diagnose presence RNA of Ebola virus, RNA of GAPDH gene, cDNA of H7N9 avian influenza virus so there is no reason why the system could not be used for DNA of *E. Coli*. Nevertheless it has to be demonstrated.

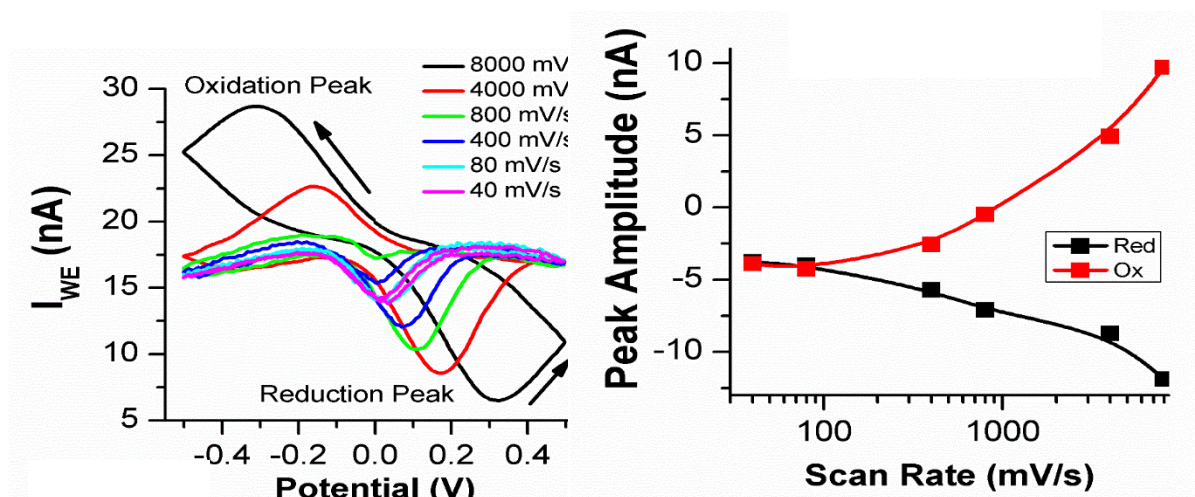


FIGURE 44 RESULTS FROM A TYPICAL CV SCAN IN 1 mM OF  $K_4[Fe(CN_6)]$  SOLUTION SHOWING THAT THE SYSTEM WITH A SCAN RATE BELOW 100 mV/s BEHAVES IN THE SAME FASHION AS DPV. WITH THE SCAN RATE ABOVE 4 V/s, THE SYSTEM BEHAVIOR IS SIMILAR TO THAT OF STANDARD CYCLIC VOLTAMMETRY.

Currently we start a new project to develop an advanced digital PCR. It should be of similar size as the real-time PCR of 3<sup>rd</sup> generation. It will detect between 1 and four samples but in spite of a conventional real-time PCR, the digital PCR provides an absolute number of DNA copies in the sample, i.e. absolute quantification. The sample will be split into a million of individual sub-samples where the PCR will be performed. Once the reaction completed we will count number of sub-samples with positive PCR results, which is equivalent to number of DNA copies in original sample. This absolute quantification is an interesting technique to monitor e.g. treatment of HIV infection using anti-viral drugs, but conventional real-time PCR can also do this job. Not as precisely, but sometimes relative quantification performed by real-time PCR might be sufficient. Nevertheless the dPCR is a very powerful technique to detect two different DNA genes simultaneously with very different number of copies in the original sample. It is a challenging job and once the ratio is larger than 1000, it is practically impossible to detect the rare DNA by conventional real-time PCR. Once the original sample is split into a million of sub-samples, then the DNA copies are distributed through the sub-samples. The sample of getting both rare and abundant DNA into the sample sub-sample is slim. If this does happen they will be in ratio 1:1, making detection of both a simple job.

This work would probably conclude my activity in the LOC area as in the future I would prefer to focus of fundamental study of cell biology using MEMS structures. I feel there is a lot of room where we can combine both techniques to learn more from cell biology.

## 4. CONCLUSION

The work presented here for detection of infectious diseases is heavily multidisciplinary and it requires deep knowledge of many scientific and technical fields. Some of them I know better, such as micromachining technology of silicon, some of them less. My work summarized in this dissertation would have never been possible without help of many co-workers, which I greatly appreciate. Unfortunately I cannot list all of them thus only the major ones, mostly chronologically:

- Juergen Pipper, IBN, Singapore, currently Baldr Biotechnologies Pte Ltd.
- Sun Wanxin, Institute of Bioengineering and Nanotechnology, currently Bruker Asia.
- Petr Muller, IMCB, Singapore, currently Recamo, Brno, Czech Republic.
- Lukas Novák, ČVUT Praha, currently Siemens A.S.
- Julian Reboud, Institute of Microelectronics, Singapore, currently University of Glasgow.
- Wong Chee Chung, IME, Singapore, currently Becton, Dickinson & comp, Singapore.
- Soon Jeffrey B. W., IME, Singapore.
- Bojan Robert Ilic, Cornell University, USA, currently NIST, USA.
- Guiseppina Simone, KIST-Europe, Germany.
- Andreas Manz, KIST-Europe, Germany.
- Christian Ahrberg, KIST-Europe, Germany.
- Ana-Vanessa Almeida, KIST-Europe, Germany.
- Camilla C.D. Campos, KIST-Europe, Germany, currently Instituto de Química, Brazil.
- Ying Xu, Fraunhofer IBMT, Germany.

And as I said above in this section, there is many others such as my co-workers from the Institute of Microelectronics and CEITEC, both BUT, Czech Republic as well as my daughter Magdalena and wife Ying, who supported me and also helped me editing this work.

Brno, Czech Republic 19 January 2016

Pavel Neužil

## 5. REFERENCES:

- 1 Terry, S. C., Jerman, J. H. & Angell, J. B. GAS-CHROMATOGRAPHIC AIR ANALYZER FABRICATED ON A SILICON-WAFER. *Ieee Transactions on Electron Devices* **26**, 1880-1886, doi:10.1109/t-ed.1979.19791 (1979).
- 2 Manz, A., Graber, N. & Widmer, H. M. MINIATURIZED TOTAL CHEMICAL-ANALYSIS SYSTEMS - A NOVEL CONCEPT FOR CHEMICAL SENSING. *Sensors and Actuators B-Chemical* **1**, 244-248, doi:10.1016/0925-4005(90)80209-i (1990).
- 3 Manz, A. *et al.* MINIATURIZATION OF CHEMICAL-ANALYSIS SYSTEMS - A LOOK INTO NEXT CENTURY TECHNOLOGY OR JUST A FASHIONABLE CRAZE. *Chimia* **45**, 103-105 (1991).
- 4 Manz, A. *et al.* MICROMACHINING OF MONOCRYSTALLINE SILICON AND GLASS FOR CHEMICAL-ANALYSIS SYSTEMS - A LOOK INTO NEXT CENTURY TECHNOLOGY OR JUST A FASHIONABLE CRAZE. *Trac-Trends in Analytical Chemistry* **10**, 144-149, doi:10.1016/0165-9936(91)85116-9 (1991).
- 5 Manz, A. *et al.* PLANAR CHIPS TECHNOLOGY FOR MINIATURIZATION AND INTEGRATION OF SEPARATION TECHNIQUES INTO MONITORING SYSTEMS - CAPILLARY ELECTROPHORESIS ON A CHIP. *Journal of Chromatography* **593**, 253-258, doi:10.1016/0021-9673(92)80293-4 (1992).
- 6 Harrison, D. J., Manz, A., Fan, Z. H., Ludi, H. & Widmer, H. M. CAPILLARY ELECTROPHORESIS AND SAMPLE INJECTION SYSTEMS INTEGRATED ON A PLANAR GLASS CHIP. *Analytical Chemistry* **64**, 1926-1932, doi:10.1021/ac00041a030 (1992).
- 7 Harrison, D. J. *et al.* MICROMACHINING A MINIATURIZED CAPILLARY ELECTROPHORESIS-BASED CHEMICAL-ANALYSIS SYSTEM ON A CHIP. *Science* **261**, 895-897, doi:10.1126/science.261.5123.895 (1993).
- 8 Kopp, M. U., de Mello, A. J. & Manz, A. Chemical amplification: Continuous-flow PCR on a chip. *Science* **280**, 1046-1048, doi:10.1126/science.280.5366.1046 (1998).
- 9 Vogelstein, B. & Kinzler, K. W. Digital PCR. *Proceedings of the National Academy of Sciences of the United States of America* **96**, 9236-9241, doi:10.1073/pnas.96.16.9236 (1999).
- 10 Jung, W. E., Han, J., Choi, J.-W. & Ahn, C. H. Point-of-care testing (POCT) diagnostic systems using microfluidic lab-on-a-chip technologies. *Microelectronic Engineering* **132**, 46-57, doi:10.1016/j.mee.2014.09.024 (2015).
- 11 Herr, A. E. *et al.* Microfluidic immunoassays as rapid saliva-based clinical diagnostics. *Proceedings of the National Academy of Sciences* **104**, 5268-5273, doi:10.1073/pnas.0607254104 (2007).
- 12 Wikipedia, t. f. e. Bernoulli Principle.
- 13 Yager, P.
- 14 Li, X., Ballerini, D. R. & Shen, W. A perspective on paper-based microfluidics: Current status and future trends. *Biomicrofluidics* **6**, 011301-011301-011313, doi:10.1063/1.3687398 (2012).
- 15 Saiki, R. K. *et al.* ENZYMATIC AMPLIFICATION OF BETA-GLOBIN GENOMIC SEQUENCES AND RESTRICTION SITE ANALYSIS FOR DIAGNOSIS OF SICKLE-CELL ANEMIA. *Science* **230**, 1350-1354, doi:10.1126/science.2999980 (1985).
- 16 Wikipedia, t. f. e. Polymerase Chain Reaction.
- 17 Wikipedia, t. f. e. Reverse Transcription PCR.
- 18 Higuchi, R., Fockler, C., Dollinger, G. & Watson, R. KINETIC PCR ANALYSIS - REAL-TIME MONITORING OF DNA AMPLIFICATION REACTIONS. *Bio-Technology* **11**, 1026-1030, doi:10.1038/nbt0993-1026 (1993).
- 19 Sciences, R. L. LightCycler® 1536 System performance.
- 20 Guttenberg, Z. *et al.* Planar chip device for PCR and hybridization with surface acoustic wave pump. *Lab on a Chip* **5**, 308-317, doi:10.1039/b412712a (2005).

- 21 Neuzil, P., Pipper, J. & Hsieh, T. M. Disposable real-time microPCR device: lab-on-a-chip at a low cost. *Molecular Biosystems* **2**, 292-298, doi:10.1039/b605957k (2006).
- 22 Neuzil, P., Zhang, C., Pipper, J., Oh, S. & Zhuo, L. Ultra fast miniaturized real-time PCR: 40 cycles in less than six minutes. *Nucleic Acids Research* **34**, doi:10.1093/nar/gkl416 (2006).
- 23 Holland, P. M., Abramson, R. D., Watson, R. & Gelfand, D. H. Detection of specific polymerase chain reaction product by utilizing the 5'----3' exonuclease activity of *Thermus aquaticus* DNA polymerase. *Proceedings of the National Academy of Sciences of the United States of America* **88**, 7276-7280 (1991).
- 24 Zhang, C. S. & Xing, D. Miniaturized PCR chips for nucleic acid amplification and analysis: latest advances and future trends. *Nucleic Acids Research* **35**, 4223-4237, doi:10.1093/nar/gkm389 (2007).
- 25 Novak, L., Neuzil, P., Pipper, J., Zhang, Y. & Lee, S. An integrated fluorescence detection system for lab-on-a-chip applications. *Lab on a Chip* **7**, 27-29, doi:10.1039/b611745g (2007).
- 26 Pipper, J. *et al.* Catching bird flu in a droplet. *Nature Medicine* **13**, 1259-1263, doi:10.1038/nm1634 (2007).
- 27 Pipper, J., Zhang, Y., Neuzil, P. & Hsieh, T.-M. Clockwork PCR including sample preparation. *Angewandte Chemie-International Edition* **47**, 3900-3904, doi:10.1002/anie.200705016 (2008).
- 28 Neuzil, P. *et al.* Rapid detection of viral RNA by a pocket-size real-time PCR system. *Lab on a Chip* **10**, 2632-2634, doi:10.1039/c004921b (2010).
- 29 Neuzil, P. *et al.* From chip-in-a-lab to lab-on-a-chip: towards a single handheld electronic system for multiple application-specific lab-on-a-chip (ASLOC). *Lab on a Chip* **14**, 2168-2176, doi:10.1039/c4lc00310a (2014).
- 30 Neuzil, P. & Reboud, J. Palm-sized biodetection system based on localized surface plasmon resonance. *Analytical Chemistry* **80**, 6100-6103, doi:10.1021/ac800335q (2008).
- 31 Novak, L., Neuzil, P., Woon, J. S. B. & Yongjun, W. in *Sensors, 2009 IEEE*. 405-407.
- 32 Ahrberg, C. D., Ilic, B. R., Manz, A. & Neuzil, P. Handheld Real-Time PCR Device. *Lab on a Chip*, doi:10.1039/C5LC01415H (2015).
- 33 Johnson, M. <https://www.genomeweb.com/pcr/study-describes-worlds-smallest-qpcr-platform>. *GenomeWeb* (2015).
- 34 Ahrberg, C. D., Manz, A., Neuzil, P. Ebola virus detection system. ?? (2015).
- 35 Ross, D., Gaitan, M. & Locascio, L. E. Temperature measurement in microfluidic systems using a temperature-dependent fluorescent dye. *Analytical Chemistry* **73**, 4117-4123, doi:10.1021/ac010370l (2001).
- 36 Neuzil, P., Cheng, F., Soon, J. B. W., Qian, L. L. & Reboud, J. Non-contact fluorescent bleaching-independent method for temperature measurement in microfluidic systems based on DNA melting curves. *Lab on a Chip* **10**, 2818-2821, doi:10.1039/c005243d (2010).
- 37 Pribylka, A. *et al.* Fast spore breaking by superheating. *Lab on a Chip* **13**, 1695-1698, doi:10.1039/c3lc41305e (2013).
- 38 Neuzil, P., Sun, W., Karásek, T. & Manz, A. Nanoliter-sized overheated reactor. *Applied Physics Letters* **106**, 024104, doi:doi:<http://dx.doi.org/10.1063/1.4905851> (2015).
- 39 Altmeyer, M. O., Manz, A. & Neuzil, P. Microfluidic Superheating for Peptide Sequence Elucidation. *Anal Chem* **87**, 5997-6003, doi:10.1021/acs.analchem.5b00189 (2015).
- 40 Ahrberg, C. D., Manz, A. & Neuzil, P. Single Fluorescence Channel-based Multiplex Detection of Avian Influenza Virus by Quantitative PCR with Intercalating Dye. *Scientific Reports* **5**, doi:10.1038/srep11479 (2015).
- 41 Johnson, M. European Researchers Enable Single-Dye Multiplex qPCR via Melt-Curve Analysis in Each Thermal Cycle. *GenomeWeb* (2015).
- 42 Ahrberg, C. D. & Neuzil, P. Doubling Throughput of a Real-Time PCR. *Scientific Reports* **5**, 9, doi:10.1038/srep12595 (2015).



- 43 França, L. T. *et al.* A review of DNA sequencing techniques. *Quarterly Reviews of Biophysics* **35**, 169-200, doi:doi:10.1017/S0033583502003797 (2002).
- 44 Ronaghi, M., Uhlen, M. & Nyren, P. A sequencing method based on real-time pyrophosphate. *Science* **281**, 363-+, doi:10.1126/science.281.5375.363 (1998).
- 45 Ahmadian, A., Ehn, M. & Hober, S. Pyrosequencing: History, biochemistry and future. *Clinica Chimica Acta* **363**, 83-94, doi:<http://dx.doi.org/10.1016/j.cccn.2005.04.038> (2006).
- 46 Vanessa, M., Neuzil, P. pyrosequencing. *LOC* (2015).
- 47 Juskova, P., Neuzil, P., Manz, A. & Foret, F. Detection of electrochemiluminescence from floating metal platelets in suspension. *Lab on a Chip* **13**, 781-784, doi:10.1039/c2lc41086a (2013).
- 48 Simone, G. *et al.* A facile in situ microfluidic method for creating multivalent surfaces: toward functional glycomics. *Lab on a Chip* **12**, 1500-1507, doi:10.1039/c2lc21217j (2012).
- 49 Simone, G. *et al.* Protein-Carbohydrate Complex Reveals Circulating Metastatic Cells in a Microfluidic Assay. *Small* **9**, 2152-2161, doi:10.1002/smll.201202867 (2013).
- 50 Campos, C. D. M., Park, J. K., Neuzil, P., da Silva, J. A. F. & Manz, A. Membrane-free electroextraction using an aqueous two-phase system. *Rsc Advances* **4**, 49485-49490, doi:10.1039/c4ra09246e (2014).
- 51 Park, J. *et al.* Direct coupling of a free-flow isotachopheresis (FFITP) device with electrospray ionization mass spectrometry (ESI-MS). *Lab on a Chip*, doi:10.1039/C5LC00523J (2015).
- 52 Jang, M., Neuzil, P., Volk, T., Manz, A. & Kleber, A. On-chip three-dimensional cell culture in phaseguides improves hepatocyte functions in vitro. *Biomicrofluidics* **9**, 034113, doi:doi:<http://dx.doi.org/10.1063/1.4922863> (2015).
- 53 Kee, J. S., Poenar, D. P., Neuzil, P., Yobas, L. & Chen, Y. Design and fabrication of Poly(dimethylsiloxane) arrayed waveguide grating. *Optics Express* **18**, 21732-21742, doi:10.1364/oe.18.021732 (2010).
- 54 Kee, J. S., Poenar, D. P., Neuzil, P. & Yobas, L. Monolithic integration of poly(dimethylsiloxane) waveguides and microfluidics for on-chip absorbance measurements. *Sensors and Actuators B-Chemical* **134**, 532-538, doi:10.1016/j.snb.2008.05.040 (2008).
- 55 Kee, J. S., Poenar, D. P., Neuzil, P. & Yobas, L. Design and fabrication of Poly(dimethylsiloxane) single-mode rib waveguide. *Optics Express* **17**, 11739-11746, doi:10.1364/oe.17.011739 (2009).
- 56 Kee, J. S., Poenar, D. P., Neuzil, P., Yobas, L. & Ieee. *Poly(dimethylsiloxane) Waveguides Integrated with Microfluidics for Absorbance Measurement.* (2008).
- 57 Poenar, D. P., Kee, J. S., Neuzil, P. & Yobas, L. in *Nems/Mems Technology and Devices Vol. 74 Advanced Materials Research* (eds S. Teo, A. Q. Liu, H. Li, & B. Tarik) 51-54 (2009).
- 58 Neuzil, P., Giselsbrecht, S., Laenge, K., Huang, T. J. & Manz, A. Revisiting lab-on-a-chip technology for drug discovery. *Nature Reviews Drug Discovery* **11**, 620-632, doi:10.1038/nrd3799 (2012).